

# Effective Affinity for Generic Currents in Markov Processes

Adarsh Raghu<sup>1\*</sup> and Izaak Neri<sup>1†</sup>

<sup>1</sup> Department of Mathematics, King's College London, UK

\* [adarsh.raghu@kcl.ac.uk](mailto:adarsh.raghu@kcl.ac.uk), † [izaak.neri@kcl.ac.uk](mailto:izaak.neri@kcl.ac.uk)

## Abstract

We introduce an effective affinity that applies to generic currents in time-homogeneous Markov processes. This effective affinity extends a previously introduced effective affinity for currents that quantify the net transitions between two states in a Markov chain, known as edge currents. Extending the effective affinity to include generic currents is important for its application in experiments because currents of interest, like the positional currents in molecular motors, are typically not edge currents. We show that the effective affinity is a single number encapsulating several dissipative and fluctuation properties of fluctuating currents: the effective affinity determines the direction of flow of the current; the effective affinity multiplied by the current is a lower bound for the rate of dissipation; for unicyclic systems the effective affinity is the standard thermodynamic affinity; and the effective affinity constrains negative fluctuations of currents, namely, it is the exponential decay constant of the distribution of current infima. We derive the above properties by using large deviation theory and martingale theory, and we introduce a family of martingales associated with generic currents. Furthermore, we make a study of the relation between effective affinities and stalling forces in a biomechanical model of motor proteins, and we find that they are almost identical when the model is thermodynamically consistent. This brings interesting perspectives on the use of stalling forces for the estimation of dissipation.

---

## Contents

<b>1</b>	<b>Introduction</b>	<b>2</b>
<b>2</b>	<b>Markov jump processes and entropy production</b>	<b>6</b>
<b>3</b>	<b>Effective affinity from large deviations of currents</b>	<b>7</b>
3.1	Definition	7
3.2	Lower bound on dissipation	8
3.3	Limiting cases	9
3.4	Effective affinity from the tilted generator	9
<b>4</b>	<b>Effective affinity from martingale theory</b>	<b>9</b>
4.1	Derivation of the martingale property of $M_t$	10
4.2	Special cases of $M_t$	10
<b>5</b>	<b>First passage problems and extreme value statistics of currents</b>	<b>10</b>
5.1	Splitting probability	11
5.2	Thermodynamic trade off relation in first-passage setups	12

<b>6</b>	<b>Optimal currents and sufficient conditions for optimality from cycle equivalence classes</b>	<b>12</b>
6.1	Definition of cycle equivalence classes $[J]$	13
6.2	Currents in the same cycle equivalence class have the same effective affinity	14
<b>7</b>	<b>Necessary condition for optimal currents in a toy model with two cycles</b>	<b>15</b>
<b>8</b>	<b>Effective affinity for a driven Brownian particle on a ring</b>	<b>15</b>
8.1	Currents in a Brownian particle on a ring	16
8.2	Effective affinity	17
8.3	Martingale	18
8.4	Dissipation bound: all currents are optimal	18
<b>9</b>	<b>Effective affinity and stalling forces in a Kinesin-1 model</b>	<b>19</b>
9.1	Stalling forces	19
9.2	Biophysical model for Kinesin-1	20
9.3	Effective affinity equals the stalling force	21
<b>10</b>	<b>Discussion</b>	<b>23</b>
<b>A</b>	<b>Model parameters for Figure 1</b>	<b>24</b>
<b>B</b>	<b>Effective affinity for edge currents</b>	<b>24</b>
B.1	Effective affinity for edge currents	25
B.2	Martingale for edge currents	26
<b>C</b>	<b>Currents in the same cycle equivalence classes have the same effective affinity</b>	<b>27</b>
C.1	Fundamental cycle basis	27
C.2	Coefficients Theorem applied to $\tilde{\mathbf{q}}(a)$	28
C.3	Coefficients of directed cycles	28
C.4	Characteristic polynomial of $\tilde{\mathbf{q}}(a)$ as a function of the $c_\gamma$	29
<b>D</b>	<b>Model parameters for Kinesin-1 model</b>	<b>30</b>
<b>E</b>	<b>Difference between the effective affinity and the stalling force for currents that are not thermodynamically consistent</b>	<b>31</b>
	<b>References</b>	<b>33</b>

---

## 1 Introduction

The term affinity originates in chemistry, where it was used to describe the force that drives a chemical reaction (originally as vague as in the sense of the attraction between particles [1]). Its precise thermodynamic formulation as a chemical potential difference originates in the works of Théophile de Donder [2, 3] on irreversible chemical reactions. De Donder expresses the rate of entropy production in a heterogeneous, nonequilibrium system by

$$\dot{s} = \sum_{\gamma \in \mathcal{F}} \frac{a_\gamma}{k_B T_{\text{env}}} \bar{j}_\gamma \quad (1)$$

where  $\gamma$  is an index labeling the different chemical reactions that can take place,  $\mathcal{F}$  represents the set of all these reactions,  $\bar{j}_\gamma$  is the velocity of the  $\gamma$ -th reaction,  $a_\gamma$  is the corresponding affinity,  $k_B$  is the Boltzmann constant and  $T_{\text{env}}$  is the temperature; see Chapter 4 in Ref. [4] for a more extensive discussion. Equation (1) expresses the entropy production  $\dot{s}$  as a sum over the forces  $a_\gamma/(k_B T_{\text{env}})$  multiplied by their corresponding currents  $\bar{j}_\gamma$ . Such decompositions of entropy production in terms of forces and fluxes apply to a large number of nonequilibrium systems [4].

In the 1970s, a mesoscopic theory for entropy production in nonequilibrium systems, including irreversible chemical reactions, was developed based on the theory of Markov processes, see Refs. [5, 6] or Chapter 3 of Ref. [7] for a recent review. Consider a Markov chain with transition rates that satisfy the local detailed balance condition [8] (also called the generalised detailed balance condition [7]). The entropy production (1) is then described by the Schnakenberg formula [6, 7]

$$\dot{s} = \sum_{\gamma \in \mathcal{C}} a_\gamma \bar{j}_\gamma, \quad (2)$$

where now  $\gamma$  is an index that labels a basis of fundamental cycles in the graph of admissible transitions of the underlying Markov chain, where  $\bar{j}_\gamma$  is the average net rate of transitions along a single edge of the  $\gamma$ -th cycle, and  $a_\gamma$  is the corresponding cycle affinity. Importantly, all quantities in Eq. (2) admit an explicit expression in terms of the transition rates of the Markov chain [6], and hence  $\dot{s}$  is a function of the transition rates of the Markov chain. The number of terms in Eq. (2) is in general significantly larger than the number of terms in Eq. (1), as the macroscopic currents in (1) can be expressed as a linear combination of a multiple of the cycle currents in Eq. (2). Note that for isothermal systems we have  $a_\gamma = a_\gamma/(k_B T_{\text{env}})$ , relating the "de Donder" affinity  $a_\gamma$  in Eq. (1) to the Markov chain affinity  $a_\gamma$  of Eq. (2). However, the affinities  $a_\gamma$  also apply to systems in contact with multiple thermal reservoirs [9].

Currents in Markov processes have fluctuations, and the affinities  $a_\gamma$  play a role in quantifying the nonequilibrium fluctuations of currents. As was discovered in the 1990s [10], fluctuating integrated currents  $J_\gamma$  associated with the average currents  $\bar{j}_\gamma$  satisfy fluctuation relations [11, 12], including the integral relation

$$\langle e^{-\sum_{\gamma \in \mathcal{C}} a_\gamma J_\gamma} \rangle = 1, \quad (3)$$

where  $\langle \cdot \rangle$  denotes an average over repeated realisations of the process. Applying Jensen's inequality to (3) and identifying  $\langle J_\gamma \rangle = \bar{j}_\gamma t$  yields the second law of thermodynamics  $\dot{s} \geq 0$ .

For nonequilibrium processes that have one macroscopic current, the affinity  $a$  (we dropped here the  $\gamma$  index as there is only one current) captures both dissipative and fluctuation properties of the fluctuating current. Indeed, the second law of thermodynamics,  $\bar{s} = \bar{j}a > 0$ , implies that the sign of the affinity  $a$  equals the sign of the average current  $\bar{j}$ . In addition, the integral fluctuation relation  $\langle e^{-aJ} \rangle = 1$  implies that fluctuations of  $J$  that have opposite sign of  $\bar{j}$  are exponentially constrained, i.e., the probability of observing a value  $J_t < j$  is smaller or equal than  $\exp(-|aj|)$  [13].

For systems with multiple currents, the second law of thermodynamics does not determine the sign of the current from the affinity, and for multiple currents it is also unclear how the fluctuation relation (3) constrains the fluctuations of an individual current. Hence, although thermodynamic affinities are useful in understanding the implications of the second law of thermodynamics on a system's dynamics, they are in general not useful in quantifying properties of a single fluctuating current of interest. This brings us to the concept of an *effective affinity*, which is an affinity-like number that encapsulates a large number of interesting properties of fluctuating currents, even in systems with multiple currents.

The effective affinity problem is the following. Assume we observe a single fluctuating current  $J_t$  in a nonequilibrium system that has multiple currents, i.e.,  $|\mathcal{C}| > 1$ . Is there a natural

way to assign an *effective* affinity  $a^*$  to the observed current that captures the nonequilibrium properties of the current as seen from an observer that only measures this current? The effective affinity should have properties that physicists and chemists associate to affinities of currents in systems with one current. For example, the effective affinity should determine the direction of flow of the current, quantify the rate of dissipation, and it should constrain the fluctuations of the current against its average flow. In systems with one current the thermodynamic affinity has all the desired properties, and thus the effective affinity should equal the thermodynamic affinity in those cases. On the other hand, for systems with multiple currents, the effective affinity is in general different from the current's corresponding thermodynamic affinity (e.g., for systems with multiple currents, thermodynamic affinities do not determine the sign of the corresponding current).

The effective affinity problem appeared a few times before in the literature, and we provide here, to the best of our knowledge, an overview of previous work. The effective affinity was first studied in terms of the fluctuation properties of currents. Building on Ref. [14], the paper [9] defines an effective affinity for a specific class of currents that satisfy asymptotically in the limit of large times a detailed fluctuation relation. For these currents, the effective affinity is the prefactor that appears in front of the current in the exponential function that appears in the fluctuation relation. Analogously, in Ref. [15] the effective affinity is defined for an electron transport problem through the integral fluctuation relation. Note that these references define the effective affinity through fluctuation relations, but additional properties of this quantity are not explored. This changed with the recent works [16–19] that develop a theory for effective affinities of *edge currents*. These are currents that monitor the net number of transitions along a single edge of the graph of admissible transitions in a Markov chain. For edge currents, the effective affinity satisfies asymptotically an integral fluctuation relation and therefore it specifies the direction of the current, as in Refs. [9, 15]. However, two new important properties were found. First, it was found that the effective affinity multiplied by the current is a lower bound for the rate of dissipation [17, 18], and second it was shown that the effective affinity is the additional force required to stall the current [16]. Further works shows that the effective affinity defines a martingale process and determines the extreme value statistics of currents [19], and for unicyclic systems the edge effective affinity equals the thermodynamic affinity [19]. Hence, in conclusion, for the specific class of edge currents these papers demonstrate that the effective affinity encapsulates a large number of properties of fluctuating currents, and these are properties that physicists associate with affinities of currents in unicyclic systems.

So far, the question remained open whether effective affinities can be defined for *generic* fluctuating currents in Markov processes. This question is a crucial step forward in resolving the applicability of the effective affinities, as fluctuating currents in experiments, such as position of a molecular motor or the beat of a cilia [20, 21], cannot be assumed to be edge currents.

In this Paper, we define an effective affinity for *generic* currents in a Markov process, addressing the issues with the general applicability of the effective affinity. We demonstrate that the effective affinity inherits all the properties of the edge effective affinity, except for the stalling force property; nevertheless, we will derive results for the stalling force in a case study of a molecular motor that raise interesting perspectives on the relation between effective affinity and stalling forces for future research.

We summarise with more detail the properties of the effective affinity. Given a fluctuating current  $J_t$  in a Markov process  $X_t$ , we define the effective affinity  $a^*$  for generic currents through the asymptotic integral fluctuation relation

$$\lim_{t \rightarrow \infty} \langle e^{-a^* J_t} \rangle = 1, \quad (4)$$

where  $\langle \cdot \rangle$  is an average over repeated realisations of the process; note that for currents with

nonzero average values,  $\langle J_t \rangle \neq 0$ , Eq. (4) has at most one unique nonzero solution.

There are a few properties of the effective affinity that follow immediately from its definition. Notably, when the current is the stochastic entropy production [13, 22], then according to the integral fluctuation relation  $a^* = 1$  [10], and in the specific case of edge currents that count the number of transitions along a single edge of a Markov jump process, we recover the effective affinity studied in Refs. [17, 18, 23]. In addition, applying Jensen's inequality to (4) we readily obtain

$$a^* \bar{j} \geq 0, \quad (5)$$

and thus the effective affinity determines the sign of the corresponding current. Hence, from (5) it follows that the effective affinity can be seen as a force that drives a current, and it is a different quantity from the thermodynamic affinity.

The effective affinity  $a^*$  encapsulates a number of additional properties of fluctuating currents that are not immediately evident from the definition. First, we show that the effective affinity quantifies the dissipation contained in a fluctuating current. Specifically, using large deviation theory we find that

$$a^* \bar{j} \leq \dot{s}, \quad (6)$$

where  $\bar{j} = \lim_{t \rightarrow \infty} \langle J_t \rangle / t$  is the average current associated with the observed current  $J_t$ , and where  $\dot{s}$  is the average rate of dissipation. The inequality (6) is suggestive of the equalities (1) and (2). However, since the effective affinity applies to a single current, it captures in general a portion of the total dissipation, as expressed by the inequality (6). Furthermore, we identify a set of optimal currents that attain the equality in (6).

Second we show that the effective affinity constrains fluctuations of generic currents. Let us assume that  $\bar{j} > 0$  so that we can define the infimum value

$$J_{\text{inf}} := \inf \{J_t : t \geq 0\}. \quad (7)$$

It then holds that the tails of the distribution of  $J_{\text{inf}}$  are exponential with a decay constant  $a^*$ , i.e.,

$$p_{J_{\text{inf}}}(j) = \exp(a^* j [1 + o_j(1)]), \quad j \leq 0, \quad (8)$$

where  $o_j(1)$  is a function that vanishes in the limit of large  $|j|$ . The extreme value law (8) generalises the exponential law for the infimum statistics of entropy production, see Refs. [24, 25], to generic currents in Markov processes.

A last property of the effective affinity that we explore is the *stalling force* property. The stalling force is the the additional force required to stall the current, and for currents that capture the transitions along a single edge in a Markov chain the stalling force equals the effective affinity [18]. In this Paper we make a numerical study of the stalling force property in a biophysical model of a molecular motor, and we find that this property does extend to the generic case. Nevertheless, when the model is thermodynamically consistent, then the stalling force is almost equal to the effective affinity (with a relative error of the order  $10^{-3}$ ), and hence for practical purposes it can be used as an estimate for the effective affinity.

From a mathematical point of view, the effective affinity relates various concepts, including, large deviation theory, martingale theory, and extreme value statistics and splitting probabilities of currents. In large deviation theory, the effective affinity is the nonzero root of the logarithmic moment generating function, and in martingale theory the effective affinity appears as the prefactor in the exponential martingales of a current. Note that these exponential martingales are a generalisation of martingales studied previously in literature, such as, the exponentiated negative fluctuating entropy production [24, 26] and an exponential martingale related to edge currents [19]. In this Paper, we use exponential martingales of generic currents to determine the splitting probabilities of currents in first-passage problems with two

boundaries. Furthermore, we use exponential martingales to derive a thermodynamic inequality involving first-passage quantities that expresses a trade off between speed, dissipation, and uncertainty [27].

The paper is structured as follows: In Sec. 2, we describe the general setup of Markov jump processes that we will be working with for most of the paper. In Sec. 3, we define the effective affinity with large deviation theory, and we use large deviation theory to derive the bound (6). In Sec. 4, we relate the effective affinity with martingale theory by defining a martingale associated with a generic fluctuating current, and in Sec. 5 we use martingale theory to derive the infimum law (8), linking the effective affinity with the current's extreme value statistics. In Sec. 6, we derive a sufficient condition for optimal currents (these are currents that attain the equality in (Eq. 6)) and this leads us to the concept of cycle equivalence classes. In the following three sections, we will explore questions related to effective affinity that are not generically addressed in this paper. Instead, we will examine these problems through case studies. In Sec. 7, we numerically investigate the optimal currents in a simple model with two cycles with the aim of identifying necessary conditions for current optimality. In Sec. 8, we make a brief detour in Markov processes on continuous state spaces. We explore the effective affinity for a particle subject to a constant force and undergoing overdamped diffusion. Last but not least, in Sec. 9 we analyse the effective affinity in a biochemical model of the molecular motor Kinesin-1, and we demonstrate that the effective affinity is the stalling force when the model is thermodynamically consistent. We end the paper with a Discussion in Sec. 10 and four appendices with technical details.

## 2 Markov jump processes and entropy production

For simplicity, we focus in this Paper on Markov jump processes in a discrete state space. We consider time-homogeneous Markov jump processes  $X_t \in \mathcal{X}$  on a finite set  $\mathcal{X}$ , which are defined by their  $\mathbf{q}$ -matrix [28, 29]. The off-diagonal entries  $\mathbf{q}_{xy}$  denote the rate at which  $X_t$  jumps from  $x$  to  $y$ , with  $x, y \in \mathcal{X}$ . The diagonal entries  $\mathbf{q}_{xx} = -\sum_{y \in \mathcal{X} \setminus \{x\}} \mathbf{q}_{xy}$  denote the exit rates out of the state  $x$ . The probability mass function  $p_t(x)$  of  $X_t$  solves the differential equation

$$\partial_t p_t(x) = \sum_{y \in \mathcal{X}} p_t(y) \mathbf{q}_{yx}. \quad (9)$$

The stationary state  $p_{ss}(x)$  is the left eigenvector of  $\mathbf{q}$  associated with its Perron root (the Perron root is the eigenvalue with the largest real part). We assume that  $X_t$  is ergodic, so that  $p_{ss}$  is unique and  $p_{ss}(x) > 0$  [30].

Fluctuating integrated currents  $J_t$  are time-extensive and time-reversal antisymmetric, fluctuating observables. Any such observable defined on a Markov jump process  $X_t$  can be expressed as a linear combination

$$J_t := \sum_{x, y \in \mathcal{X}} c_{xy} J_t^{xy} \quad (10)$$

of edge currents  $J_t^{xy}$ , which are defined as the difference between the number of forward jumps  $N_t^{xy}$  and the number of backward jumps  $N_t^{yx}$  between  $x$  and  $y$  in the interval  $[0, t]$ , i.e.,

$$J_t^{xy} := N_t^{xy} - N_t^{yx}. \quad (11)$$

The coefficients  $c_{xy} = -c_{yx} \in \mathbb{R}$  quantify the flow of the transported resource when the process jumps from  $x$  to  $y$ . When  $\mathbf{q}_{xy} = 0$ , then the corresponding coefficient  $c_{xy}$  is irrelevant. Therefore, the relevant coefficients  $c_{xy}$  span an Euclidean space of dimension  $|\mathcal{E}|$ , where  $\mathcal{E}$  is

the set of nondirected edges in the graph of admissible transitions (i.e., the pairs  $(x, y)$  with  $\mathbf{q}_{xy} \neq 0$ ). The corresponding average current  $\bar{j}$  takes the expression

$$\bar{j} := \lim_{t \rightarrow \infty} \langle J_t \rangle / t = \sum_{x \in \mathcal{X}} \sum_{y \in \mathcal{X} \setminus \{x\}} c_{xy} \bar{j}_{xy}, \quad (12)$$

where

$$\bar{j}_{xy} := \lim_{t \rightarrow \infty} \langle J_t^{xy} \rangle / t = p_{ss}(x) \mathbf{q}_{xy} - p_{ss}(y) \mathbf{q}_{yx} \quad (13)$$

is the average of the edge current associated with the transition between states  $x$  and  $y$ . Without loss of generality, we assume in this Paper that  $\bar{j} > 0$ .

An important example of a fluctuating current is the fluctuating entropy production [7, 13, 22],

$$S_t := \frac{1}{2} \sum_{x \in \mathcal{X}} \sum_{y \in \mathcal{X} \setminus \{x\}} J_t^{xy} \ln \frac{p_{ss}(x) \mathbf{q}_{xy}}{p_{ss}(y) \mathbf{q}_{yx}}, \quad (14)$$

which is the fluctuating current with coefficients  $c_{xy}$  that are equal to the microscopic edge affinities  $c_{xy} = \ln \frac{p_{ss}(x) \mathbf{q}_{xy}}{p_{ss}(y) \mathbf{q}_{yx}}$ . Using the principle of local detailed balance, we can identify the average rate

$$\dot{s} := \lim_{t \rightarrow \infty} \langle S_t \rangle / t = \frac{1}{2} \sum_{x \in \mathcal{X}} \sum_{y \in \mathcal{X} \setminus \{x\}} \bar{j}_{xy} \ln \frac{p_{ss}(x) \mathbf{q}_{xy}}{p_{ss}(y) \mathbf{q}_{yx}} \quad (15)$$

with the rate of dissipation [8]. The rate of dissipation  $\dot{s}$  can also be expressed as a sum of the form Eq. (2) where the  $\gamma$  are cycles of a fundamental cycle basis  $\mathcal{C}$ , where  $\bar{j}_\gamma$  is the current along an edge of the cycle  $\gamma$ , and where

$$a_\gamma = \ln \frac{\prod_{(x,y) \in \gamma} \mathbf{q}_{xy}}{\prod_{(x,y) \in -\gamma} \mathbf{q}_{xy}} \quad (16)$$

are the cycle affinities; we have used  $-\gamma$  for the cycle obtained from  $\gamma$  by changing the orientation of the edges.

### 3 Effective affinity from large deviations of currents

We initiate our study of the effective affinity in large deviation theory, where it naturally appears as the non-zero root of the logarithmic moment generating function.

#### 3.1 Definition

Currents of the form (10) satisfy a large deviation principle when  $\bar{j} \neq 0$  [31–33]. Indeed, the probability distribution of  $J_t/t$  takes for large values of  $t$  the form

$$p_{J_t/t}(j) = \exp(-t\mathcal{I}(j)[1 + o_t(1)]), \quad (17)$$

where  $\mathcal{I}(j)$  is the rate function of  $J_t$  and  $o_t(1)$  denotes an arbitrary function that converges to zero for large values of  $t$ . According to the Gärtner-Ellis theorem [34, 35],  $\mathcal{I}(j)$  is the Legendre-Fenchel transform of the logarithmic moment generating function

$$\lambda_J(a) := \lim_{t \rightarrow \infty} \frac{1}{t} \ln \langle e^{-aJ_t} \rangle \quad (18)$$

such that

$$\mathcal{I}_J(j) = \max_a (-\lambda_J(a) - aj). \quad (19)$$

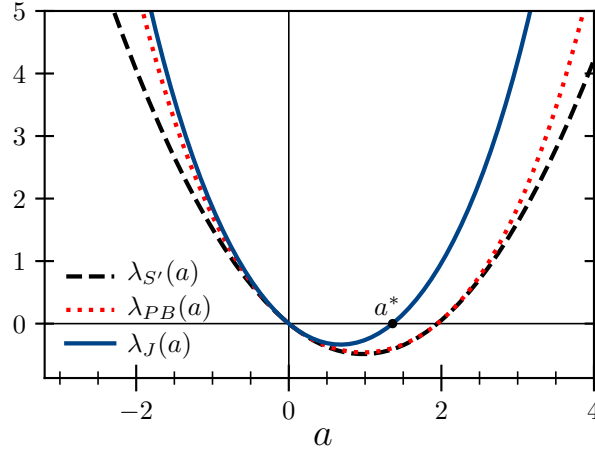


Figure 1: *Illustrated definition of the effective affinity  $a^*$ .* The logarithmic moment generating function  $\lambda_J$  is plotted as a function of  $a$  for an example current  $J$  in the four state model of Fig. 3 (see Appendix A for definitions). The effective affinity  $a^*$ , defined as the nonzero root of  $\lambda_J(a)$ , is marked by a circle. In addition, the logarithmic moment generating function  $\lambda_{S'}$  for the rescaled fluctuating entropy production  $S' = S/\dot{s}$ , and the parabola  $\lambda_{PB}(a) = a\bar{j}(-1 + a\bar{j}/\dot{s})$  that appears on the right hand side of the inequality (22) are plotted as a function of  $a$ . Note that in both cases ( $J_t$  and  $S'_t$ ) the average current equals 1.

We define the effective affinity  $a^*$  as the nonzero root of  $\lambda_J(a)$  (see Fig. 1 for an illustration), i.e.,

$$\lambda_J(a^*) = 0, \quad (20)$$

a definition that is consistent with Eq. (4). If  $\bar{j} = 0$ , then  $\lambda_J(a)$  has no nonzero root, and we define  $a^* = 0$ . Notice that the cumulants of  $J_t/t$  are determined by the derivatives of  $\lambda_J(a)$  at the zero root,  $a = 0$ . Instead in this paper, we highlight the importance of the second root  $a^*$  of the logarithmic moment generating function that captures atypical properties of  $J$ .

Applying Jensen's inequality to Eq. (4) we find

$$a^*\bar{j} \geq 0. \quad (21)$$

Hence,  $a^*$  has the same sign as  $\bar{j}$  and therefore we can say that the effective affinity sets the direction in which the current flow. Note that this property does not hold for the thermodynamic affinities in Eq. (1), and the effective affinity is thus in general different from the thermodynamic affinity.

### 3.2 Lower bound on dissipation

The effective affinity multiplied by the average current captures a portion of the entropy production rate of the system as expressed by the inequality Eq. (6), i.e.,  $\dot{s} \geq a^*\bar{j}$ . This is one of the main properties of the effective affinity, and we derive it here from large deviation theory.

The inequality (6) follows from the universal lower bound

$$\lambda_J(a) \geq a\bar{j} \left( -1 + a\frac{\bar{j}}{\dot{s}} \right), \quad (22)$$

on the logarithmic moment generating function of  $J_t$ . The parabolic bound (22) was conjectured in [36] for arbitrary currents  $J_t$  in Markov jump processes based on substantial numerical



evidence, and subsequently derived in Ref. [37] by applying the contraction principle to the level 2.5 large deviation rate function. Since the effective affinity  $a^*$  is the positive root of  $\lambda_J(a)$ , it is smaller or equal than the positive root  $a = \bar{s}/\bar{j}$  of the right-hand side of (22), as illustrated in Fig. 1, which concludes the derivation of the bound (6).

### 3.3 Limiting cases

We consider the effective affinity in two relevant limiting cases of the current  $J_t$ . If  $J_t = J_t^{xy}$ , then the effective affinity equals (see Appendix B.1),

$$a^* = \ln \frac{p_{ss}^{(x,y)}(x) \mathbf{q}_{xy}}{p_{ss}^{(x,y)}(y) \mathbf{q}_{yx}} \quad (23)$$

where  $p_{ss}^{(x,y)}(x)$  is the probability mass function of a modified Markov jump process for which the transition rates along the  $(x, y)$ -edge have been set to zero. On the right-hand side of Eq. (23) we recognise the effective affinity for edge currents as studied in Refs. [16–18], and hence  $a^*$  extends the effective edge affinity (23) to generic currents in Markov processes.

Another interesting limiting case is when  $J_t = kS_t$  with  $k \in \mathbb{R}$ . Such currents satisfy the Gallavotti-Cohen symmetry [10]

$$\lambda_J(a) = \lambda_J(k^{-1} - a), \quad (24)$$

and thus  $a^* = 1/k$ . In addition, since  $\bar{j} = k\bar{s}$ , the equality in (6) is attained [27] for currents that are proportional to the stochastic entropy production.

### 3.4 Effective affinity from the tilted generator

For Markov processes defined on finite sets, we can readily obtain  $\lambda_J(a)$ , and thus also the effective affinity  $a^*$ , from the spectrum of a “tilted”  $\mathbf{q}$ -matrix. Indeed, applying Kolmogorov’s backward equation to  $\langle e^{-aJ_t} \rangle$ , it follows that  $\lambda_J(a)$  is the Perron root of the tilted matrix [34,38]

$$\tilde{\mathbf{q}}_{xy}(a) = \begin{cases} \mathbf{q}_{xy} e^{-ac_{xy}}, & \text{if } x \neq y, \\ -\sum_{z \in \mathcal{X} \setminus \{x\}} \mathbf{q}_{xz}, & \text{if } x = y. \end{cases} \quad (25)$$

The effective affinity  $a^*$  is thus the value of  $a$  at which the Perron root vanishes, and obtaining  $a^*$  is thus a straightforward computation when the set  $\mathcal{X}$  is finite.

## 4 Effective affinity from martingale theory

Let  $M_t$  be a stochastic process that is a function of the trajectory of  $X$  in the interval  $[0, t]$ . The process  $M_t$  is a martingale if it has no drift, i.e.,

$$\langle M_t | X_0^s \rangle = M_s \quad (26)$$

for all  $s \in [0, t]$ , where  $\langle \cdot | X_0^s \rangle$  denotes the expectation conditioned on the trajectory of  $X_t$  in the interval  $[0, s]$ .

We show in this section that the process

$$M_t := \phi_{a^*}(X_t) e^{-a^* J_t} \quad (27)$$

is a martingale, where  $\phi_a(x)$  is the right eigenvector of the Perron root of the tilted matrix  $\tilde{\mathbf{q}}(a)$ . Note that the effective affinity  $a^*$  appears as the prefactor of  $J_t$  in the exponential martingale (27), and hence effective affinities also play a role in martingale theory for generic currents.

#### 4.1 Derivation of the martingale property of $M_t$

The martingality of  $M_t$  follows from the fact that  $\phi_{a^*}(x)e^{-a^*j}$  is a harmonic function of the generator of the joint process  $(X_t, J_t)$ .

The function

$$f_t(x, j) = \langle \phi_{a^*}(X_t) e^{-a^*J_t} | X_0 = x, J_0 = j \rangle, \quad (28)$$

solves the Kolmogorov backward equation of the joint process  $(X_t, J_t)$ , i.e.,

$$\partial_t f_t(x, j) = \sum_{y \in \mathcal{X}} \mathbf{q}_{xy} [f_t(y, j + c_{xy}) - f_t(x, j)], \quad (29)$$

with initial condition

$$f_0(x, j) = \phi_{a^*}(x) e^{-a^*j}. \quad (30)$$

The process  $M_t$  is a martingale if  $\partial_t f_t(x, j) = 0$ , see Ref. [39], which requires that  $f_0(x, j)$  is a harmonic function of the joint process  $(X, J)$ , i.e.,

$$\sum_{y \in \mathcal{X}} \mathbf{q}_{xy} [f_0(y, j + c_{xy}) - f_0(x, j)] = 0. \quad (31)$$

Using (30), we find that (31) holds when

$$\sum_{y \in \mathcal{X}} \tilde{\mathbf{q}}_{xy}(a^*) \phi_{a^*}(y) = 0, \quad (32)$$

which implies that  $\phi_{a^*}(x)$  is a right eigenvector of the tilted matrix  $\tilde{\mathbf{q}}_{xy}(a^*)$  associated with a zero root.

#### 4.2 Special cases of $M_t$

Equation (27) describes a family of martingales for different currents  $J_t$ , which reduce in special cases of specific currents to known Martingales in Markov processes. [39]. Notably, for  $J_t = S_t$  we get  $M_t = \exp(-S_t)$ , as  $a^* = 1$  and  $\phi_{a^*} = 1$ , and thus we recover that the exponentiated negative entropy production is a martingale [24, 26]. Another limiting case is when  $J_t = J_t^{x \rightarrow y}$ , the edge current between states  $x, y \in \mathcal{X}$  (the edge current can be obtained from Eq. (10) by setting  $c_{ab} = \delta_{a,x} \delta_{b,y} - \delta_{a,y} \delta_{b,x}$ , where  $\delta_{a,b}$  is the Kronecker delta function). In this case, the martingale  $M_t$ , given by Eq. (27), is equivalent to the martingale in Eq. (69) of Ref. [19], as we show in Appendix B.2. This follows from the fact that for edge currents  $a^*$  is given by Eq. (23) and the right null eigenvector  $\phi_{a^*}$  equals  $p_{ss}^{(x,y)}$  (see the Supplementary Material in Ref. [16]).

## 5 First passage problems and extreme value statistics of currents

We revisit the first passage problem of a fluctuating current  $J_t$  exiting an open interval  $(-\ell_-, \ell_+)$  as studied in Ref. [27]. The first passage time is defined by

$$T := \min \{ t \geq 0 : J_t \notin (-\ell_-, \ell_+) \}. \quad (33)$$

This is a generalisation of the gambler's ruin problem, as introduced by Pascal in the 17th century [40, 41], that applies to fluctuating currents [42].

The splitting probability  $p_-$ , corresponding with the probability of ruin in the gambler's ruin problem, is the probability that the current first exits the interval  $(-\ell_-, \ell_+)$  from the negative threshold, namely,

$$p_- := P(J_T \leq -\ell_-), \quad (34)$$

where the symbol  $P$  denotes the probability of an event.

Using the martingale  $M_t$ , we show in Sec. 5.1 that the effective affinity is the decay constant determining the exponential decay of  $p_-$  with  $\ell_-$ , i.e.,

$$\lim_{\ell_- \rightarrow \infty} \frac{|\ln p_-|}{\ell_-} = a^*. \quad (35)$$

As a corollary of this result, we find that  $a^*$  is also the exponential decay constant of the distribution of current infima  $J_{\text{inf}}$ , see Eq. (8), relating large deviation theory extreme value statistics. Next, in Sec. 5.2 we use martingales to derive the inequality in Ref. [27] between the rate of dissipation, the mean-first passage time, the splitting probability, and the thresholds. Although this inequality was presented before, the derivation we present here is new and is arguably more transparent (it does not involve scaling arguments as in [27]).

### 5.1 Splitting probability

Since  $\langle J_t \rangle > 0$ , and since the interval  $(-\ell_-, \ell_+)$  is finite, the first-passage time  $T$  is with probability one finite, which implies that

$$p_- + p_+ = 1, \quad (36)$$

where  $p_+ = P(J_T \geq \ell_+)$  and  $p_- = P(J_T \leq -\ell_-)$  are the probabilities that the current  $J_t$  exits the interval  $(-\ell_-, \ell_+)$  from the negative or positive thresholds, respectively.

According to Doob's Optional Stopping Theorem, see Refs. [25, 43], a martingale  $M_t$  has the following property

$$\langle M_T \rangle = \langle M_0 \rangle, \quad (37)$$

if  $T$  is with probability one finite and  $|M_T| \leq \max\{\ell_-, \ell_+\}$ . Substitution of Eq. (27) in Doob's Optional Stopping Theorem yields

$$\begin{aligned} & \langle \phi_{a^*}(X_T) \exp(-a^* J_T) \rangle \\ &= p_- e^{a^* \ell_- (1+o_{\ell_{\min}}(1))} \langle \phi_{a^*}(X_T) \rangle_- + p_+ e^{-a^* \ell_+ (1+o_{\ell_{\min}}(1))} \langle \phi_{a^*}(X_T) \rangle_+ \\ &= \langle \phi_{a^*}(X_0) \rangle = 1, \end{aligned} \quad (38)$$

where  $\langle \cdot \rangle_+$  and  $\langle \cdot \rangle_-$  are expectations over repeated realisations of the process  $X_t$  conditioned on the event that  $J_T \geq \ell_+$  or  $J_T \leq -\ell_-$ , respectively, and where  $o_{\ell_{\min}}(1)$  represents an arbitrary function that decays to zero when  $\ell_{\min} = \min\{\ell_-, \ell_+\}$  diverges. We have used  $J_T = \ell_{\pm}(1 + o_{\ell_{\min}}(1))$ , as the increments of  $J_t$  are bounded and independent of  $\ell_-$  and  $\ell_+$ . In addition, note that, without loss of generality, we have set  $\langle \phi_{a^*}(X_0) \rangle = 1$ , as  $\phi_{a^*}(x)$  is a right eigenvector of  $\tilde{\mathbf{q}}(a^*)$ , and it is thus defined up to an arbitrary constant. Solving Eqs. (36) and (38) towards  $p_-$  yields

$$p_- = \frac{1 - e^{-a^* \ell_+ (1+o_{\ell_{\min}}(1))} \langle \phi_{a^*}(X_T) \rangle_+}{e^{a^* \ell_- (1+o_{\ell_{\min}}(1))} \langle \phi_{a^*}(X_T) \rangle_- - e^{-a^* \ell_+ (1+o_{\ell_{\min}}(1))} \langle \phi_{a^*}(X_T) \rangle_+}. \quad (39)$$

Taking the limits  $\ell_-, \ell_+ \rightarrow \infty$ ,  $\ln \langle \phi_{a^*}(X_T) \rangle_{\pm}$  can be contained in the correction term  $o_{\ell_{\min}}(1)$ , as the set  $\mathcal{X}$  is finite and  $|\phi_{a^*}(x)|$  is bounded and independent of the thresholds  $\ell_-$  and  $\ell_+$  and this yields us the formula (35) that we were meant to derive.

In the limit of  $\ell_+ \rightarrow \infty$ , the splitting probability  $p_-$  is the cumulative distribution of  $J_{\text{inf}}$ , i.e.,

$$P(J_{\text{inf}} \leq \ell_-) = \lim_{\ell_+ \rightarrow \infty} p_-(\ell_-), \quad (40)$$

and Eq. (35) combined with Eq. (40) yields the result (8) for the infimum statistics of  $J$ .

## 5.2 Thermodynamic trade off relation in first-passage setups

The inequality (6) combined with the martingale result (35) implies a trade off relation between dissipation ( $\dot{s}$ ), speed ( $\langle T \rangle$ ), and uncertainty ( $|\ln p_-|$ ). Indeed, using Eq. (35) and Wald's equality for fluctuating currents [44, 45],

$$\bar{j} = \frac{\ell_+}{\langle T \rangle} (1 + o_{\ell_{\min}}(1)), \quad (41)$$

in the inequality (6), yields

$$\dot{s} \geq \frac{\ell_+}{\ell_-} \frac{|\ln p_-|}{\langle T \rangle} (1 + o_{\ell_{\min}}(1)). \quad (42)$$

The trade off inequality (42) applies to physical processes with a finite termination time. An example is a molecular motor that moves on a one-dimensional substrate and detaches from this substrate once it reaches one of its two end points, which we label by the + and – end points. Assuming that the motor is biased towards the + end point, then  $p_-$  quantifies the probability of reaching the wrong end point,  $\langle T \rangle$  is the average duration of the process, and  $\dot{s}$  is the rate of dissipation. Hence, in this example Eq. (42) expresses a trade off between the error, the speed, and the rate of dissipation.

Replacing the quantities  $\langle T \rangle$  and  $p_-$  in the right-hand side of Eq. (42) with their empirical estimates, we obtain an estimator for  $\dot{s}$ . The bias of this estimator is given by  $\dot{s} - \hat{s}_{\text{FPR}}$ , with

$$\hat{s}_{\text{FPR}} := \frac{\ell_+}{\ell_-} \frac{|\ln p_-|}{\langle T \rangle} \quad (43)$$

the first-passage ratio [46]. In previous works, the first-passage ratio was obtained by numerically solving recursion relations for  $p_-$  at finite thresholds  $\ell_-$  and  $\ell_+$  [46]. Instead, here we have shown that

$$\hat{s}_{\text{FPR}} = \bar{j} a^*, \quad (44)$$

and hence the bias in the estimator can readily be obtained from diagonalising the tilted matrix  $\tilde{\mathbf{q}}(z)$ .

## 6 Optimal currents and sufficient conditions for optimality from cycle equivalence classes

We say that a current  $J_t$  is *optimal* if the equalities in the bounds (6) and (42) are attained. For optimal currents, the effective affinity captures all the dissipation in the process  $X_t$ , and hence estimates of dissipation based on the first-passage ratio are unbiased. Optimal currents are also relevant for systems that want to optimise the trade off between dissipation, speed, and uncertainty, as expressed in Eq. (42).

The stochastic entropy production  $S_t$  is an example of an optimal current, as in Sec. 3.3 we have shown that the equality in the bounds (6) and (42) are attained for currents of the form  $J_t = kS_t$ , with  $k$  a constant. In this section, we extend significantly this result by introducing cycle equivalence classes.

First, in Sec. 6.1, we partition the set  $\mathcal{J}$  of all currents  $J_t$  into cycle equivalence classes  $[J_t]$ . The cycle equivalence classes are defined so that all currents in the same equivalence class have the same set of cycle coefficients  $c_\gamma$ , with  $\gamma$  the fundamental cycles that are part of the fundamental cycle basis  $\gamma \in \mathcal{C}$ . The cycle coefficients  $c_\gamma$  are known in the statistical physics literature from Schnakenberg's network theory [6, 47], and we review some relevant parts of this theory also in Sec. 6.1. Next, in Sec. 6.2 we show that all currents that are part

of the same cycle equivalence class  $[J_t]$  have the same effective affinity  $a^*$ . Therefore, the optimality property of  $kS_t$  extends to all currents that belong to the cycle equivalence classes  $[kS_t]$ . Note that equivalence classes are sets of currents that are isomorphic to  $\mathbb{R}^{|\mathcal{X}|-1}$ , and all the currents in the sets  $[kS_t]$  are optimal in the sense that the equalities in the Eqs. (6) and (42) are attained.

### 6.1 Definition of cycle equivalence classes $[J]$

Let  $\mathcal{G} = (\mathcal{X}, \mathcal{E})$  be the graph of admissible transitions of the Markov jump process  $X$  defined by  $\mathbf{q}$ . As detailed in Appendix C.1, we can construct a fundamental cycles basis  $\mathcal{C}$  that spans the cycle space of the graph  $\mathcal{G}$  (any cycle in the graph of admissible transitions can be obtained as a symmetric difference of the fundamental cycles  $\gamma \in \mathcal{C}$ ). The cycles in  $\mathcal{C}$  are sequences of nonrepeating vertices  $[x_1(\gamma), x_2(\gamma), \dots, x_{n(\gamma)}(\gamma), x_1(\gamma)]$ , where  $n(\gamma)$  is the number of distinct vertices in  $\gamma$  and the  $x_i$  are the vertices visited in the cycle.

Currents  $J_t$  in the process  $X$  are determined by the coefficients  $c_{xy}$  with  $(x, y) \in \mathcal{E}$  [see Eq. (10)]. Given a fluctuating current, we define its cycle coefficients  $c_\gamma$  by

$$c_\gamma := \sum_{i=1}^{n(\gamma)} c_{x_i x_{i+1}}, \quad \gamma \in \mathcal{C}, \quad (45)$$

where the  $x_i$  are the vertices of  $\gamma$ , and it should be understood that  $x_{n(\gamma)+1} = x_1$ .

The cycle coefficients  $c_\gamma$  are known from Schnakenberg's network theory, viz., the coefficients  $c_\gamma$  appear when expressing the steady state currents in a Markov process as linear combinations of the *cycle currents* associated with the fundamental cycles  $\gamma \in \mathcal{C}$  [6, 47], which we will define next. At stationarity,  $\partial_t p_t(x) = 0$ , and hence (9) implies that

$$\sum_{y \in \mathcal{X}: (x, y) \in \mathcal{E}} \bar{j}_{xy} = 0, \quad (46)$$

which we recognise as Kirchhoff's first law applied to each state  $x \in \mathcal{X}$ . This set of  $|\mathcal{X}|$  equations imposes  $|\mathcal{X}| - 1$  linearly independent constraints on the edge currents  $\bar{j}_{xy}$  (and not  $|\mathcal{X}|$  constraints as  $\sum_{x \in \mathcal{X}} p_t(x)$  must be constant in time). Consequently the number of independent currents required to describe all the edge currents is  $|\mathcal{C}| = |\mathcal{E}| - |\mathcal{X}| + 1$ . We choose  $|\mathcal{C}|$  such currents by associating to each fundamental cycle  $\gamma \in \mathcal{C}$  a current  $\bar{j}_\gamma$  such that

$$\bar{j}_{xy} = \sum_{\gamma \in \mathcal{C}} \eta_{x,y,\gamma} \bar{j}_\gamma, \quad (47)$$

where  $\eta_{x,y,\gamma} = 0$  if the edge  $(x, y)$  is not in the cycle  $\gamma$ , and  $\eta_{x,y,\gamma} = +1(-1)$  if the edge  $(x, y)$  is in the cycle and the node  $x$  appears before (after) the node  $y$  in the cycle  $\mathcal{C}$ , (where we use the same direction assumed in the sum in Eq. (45)). This set of  $|\mathcal{E}|$  equations can be reduced using the constraints (46) to a set of  $|\mathcal{E}| - |\mathcal{X}| + 1 = |\mathcal{C}|$  independent equations that can be solved towards the  $|\mathcal{C}|$  cycle currents  $\bar{j}_\gamma$ .

Thus for a given Markov process, after choosing a fundamental cycle basis  $\mathcal{C}$ , and for each  $\gamma \in \mathcal{C}$  associating the corresponding cycle current  $\bar{j}_\gamma$  by solving the equations (47), and cycle coefficients  $c_\gamma$  for a fluctuating current  $J_t$  by Eq. (45), then using these and Eq. (12) the average current  $\bar{j}$  associated with  $J_t$  is expressible as

$$\bar{j} = \sum_{\gamma \in \mathcal{C}} c_\gamma \bar{j}_\gamma. \quad (48)$$

Therefore the coefficients  $c_\gamma$  are sufficient to determine the current  $\bar{j}$  associated with a fluctuating current  $J_t$ .

The cycle equivalence classes that we use in this paper are the set of currents  $[J_t]$  that have the same cycle coefficients  $c_\gamma$  as the current  $J_t$ . Note that the set  $\mathcal{J}$  of all currents is isomorphic to the Euclidean space  $\mathbb{R}^{|\mathcal{E}|}$ . Since there are a number  $|\mathcal{C}| = |\mathcal{E}| - |\mathcal{X}| + 1$  of cycle coefficients (see Appendix C.1), the cycle equivalence classes are isomorphic to  $\mathbb{R}^{|\mathcal{X}|-1}$ . In the next section, we show that all fluctuating currents  $J_t$  within a cycle equivalence class have the same effective affinity, which is our interest in these equivalence classes.

## 6.2 Currents in the same cycle equivalence class have the same effective affinity

We show that all currents in the same equivalence class  $[J_t]$  have the same logarithmic moment generating function  $\lambda_J(a)$ , and hence also the same effective affinity  $a^*$ . To this aim, we show that  $\lambda_J(a)$  depends on the coefficients  $c_{xy}$  through the cycle coefficients  $c_\gamma$ .

Since  $\lambda_J(a)$  is the Perron root of  $\tilde{\mathbf{q}}(a)$ , it is sufficient to demonstrate that the characteristic polynomial of the tilted matrix  $\tilde{\mathbf{q}}(a)$  depends on the coefficients  $c_{xy}$  through the cycle coefficients  $c_\gamma$ . To show this latter, we consider a graphical expansion of the characteristic polynomial of  $\tilde{\mathbf{q}}(a)$  in terms of the spanning, linear subgraphs of the graph of admissible transitions,  $\mathcal{G} = (\mathcal{X}, \mathcal{E})$ , of the Markov process  $X$ . We provide a formal definition of  $\mathcal{L}$  in the Appendix C.2, while here we provide an informal definition with the help of Fig. 2. A linear subgraph of the graph is a directed subgraph for which the indegree and outdegree of each node equals one, and we call the subgraph spanning when its vertex set equals  $\mathcal{X}$ . To construct the spanning, linear subgraphs of  $\mathcal{G} = (\mathcal{X}, \mathcal{E})$  we use two more conventions, namely, we consider that all nondirected edges of  $\mathcal{E}$  consist of two directed edges and we add to all nodes a self-loop (see panel (a) of Fig. 2). In Panel (b) we show an example of a spanning linear subgraph. It is the disjoint union of three kind of graphs, namely, self-loops ( $\mathbb{S}_\mathcal{L}$ ) that consist of an isolated node, double edges ( $\mathbb{E}_\mathcal{L}$ ) that consist of two nodes connected by a nondirected edge (or equivalently two directed edges), and directed simple cycles ( $\mathbb{C}_\mathcal{L}$ ).

As we show in Appendix C, the characteristic polynomial of  $\tilde{\mathbf{q}}(a)$  can be expressed as a sum over all spanning, linear subgraphs of the graph of admissible transitions in the Markov process  $X$ , viz.,

$$\det(\tilde{\mathbf{q}}(a) - \xi \mathbb{1}) = \sum_{\mathcal{L}} (-1)^{|\mathcal{X}| + \kappa(\mathcal{L})} \left( \prod_{(x,x) \in \mathbb{S}_\mathcal{L}} (\mathbf{q}_{xx} - \xi) \right) \left( \prod_{\{(x \rightarrow y), (y \rightarrow x)\} \in \mathbb{E}_\mathcal{L}} \mathbf{q}_{yx} \mathbf{q}_{xy} \right) \left( \prod_{\mathcal{C} \in \mathbb{C}_\mathcal{L}} \exp(\mathcal{A}_\mathcal{C}) \exp\left(-a \sum_{\mathcal{C}_i \in \mathcal{C}} \epsilon_{\mathcal{C}_i, \gamma} c_\gamma\right) \right), \quad (49)$$

where  $\det(\cdot)$  denotes the determinant of a matrix, where  $\kappa(\mathcal{L})$  is the number of strongly connected components in the spanning linear subgraph  $\mathcal{L}$ , and where  $\mathbb{1}$  is the identity matrix of order  $|\mathcal{X}|$ . The Eq. (49) follows from the Coefficients Theorem for Directed Graphs [48], see Appendix C.

It readily follows from Eq. (49) that the dependency of the characteristic polynomial of  $\tilde{\mathbf{q}}(a)$  on the coefficients  $c_{xy}$  is through the cycle coefficients  $c_\gamma$ , and therefore all currents in  $[J_t]$  share the same effective affinity. In addition, in Appendix C.4 we show that all currents in  $[S_t]$  satisfy the Galavotti-Cohen symmetry, and thus the optimality of a current is related to the Galavotti-Cohen symmetry.

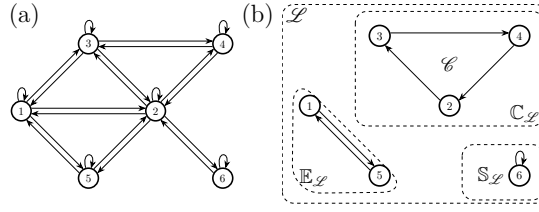


Figure 2: Example of a spanning linear subgraph  $\mathcal{L}$  as used in the graphical expansion of the characteristic polynomial of  $\tilde{\mathbf{q}}$  in Eq. (49). Panel (a) shows an example of a graph of admissible transitions  $\mathcal{G} = (\mathcal{X}, \mathcal{E})$  in a Markov chain with six states. For the graphical expansion we need to represent  $\mathcal{G} = (\mathcal{X}, \mathcal{E})$  as a directed graph (each nondirected edge equals two directed edges) and we need to associated to each node a self-loop. Panel (b) shows a spanning linear subgraph of the graph shown in Panel (a).

## 7 Necessary condition for optimal currents in a toy model with two cycles

Equivalence with the stochastic entropy production  $S_t$  is, up to an irrelevant proportionality constant, sufficient for optimality of a current (i.e., so that the equalities in Eqs. (6) and (42) are attained). However, the question remains whether this condition is necessary, i.e., whether the cycle equivalence classes  $[kS_t]$  contain all possible currents that attain the equalities in the bounds (6) and (42).

Here, we settle this question for models with two fundamental cycles through a numerical case study of the four state model illustrated in Fig. 3(a). The four state model has two fundamental cycles denoted by  $\gamma = 1$  and  $\gamma = 2$ , and hence the cycle equivalence classes of this model are determined by two coefficients  $c_1$  and  $c_2$ , such that  $\bar{j} = c_1 \bar{j}_1 + c_2 \bar{j}_2$ . We normalise  $c_1$  and  $c_2$  such that  $\bar{j} = 1$ . For this choice of normalisation, the dependence of  $a^*$  on the  $c_{xy}$ -coefficients that define  $J_t$  is fully determined by one parameter, namely the angle  $\alpha$  between the vectors  $(c_1, c_2)$  and  $(a_1, a_2)$ , where the latter are the cycle coefficients of  $[S_t/\dot{s}]$ ; see Fig. 3(b) for an illustration.

Figure 3(c) plots  $a^*$  as a function of  $\alpha$  for randomly generated transition rates  $\mathbf{q}$ . According to the inequality (6), which here reads  $a^*/\dot{s} \leq 1$ , the equality  $a^* = \dot{s}$  is attained when  $\alpha = 0$  or  $\alpha = \pi$ , corresponding with fluctuating currents that belong to  $[S_t/\dot{s}]$  or  $[-S_t/\dot{s}]$ , respectively. We observe that the effective affinity is a monotonously decreasing/increasing function between the value of  $\alpha$  with vanishing average current (where  $a^* = 0$ ) and the end point values  $\alpha = 0$  and  $\alpha = \pi$ . Hence, for models with two fundamental cycles, the equalities in the trade-off relations (6) and (42) are attained for currents that belong to the cycle equivalence classes  $[kS_t]$  with  $k \in \mathbb{R}$ .

In conclusion, for models with two cycles the equivalence of currents with  $S_t$  (in the sense of cycle equivalence classes) is necessary and sufficient for optimality.

## 8 Effective affinity for a driven Brownian particle on a ring

Thus far, we have focused on Markov processes defined on a discrete set  $\mathcal{X}$ . Nevertheless, the definition of the effective affinity, Eq. (20), and its ensuing properties — amongst others, the bound (6), the infimum statistics results (8), and the martingale  $M_t$  (27) — also apply to driven diffusions.

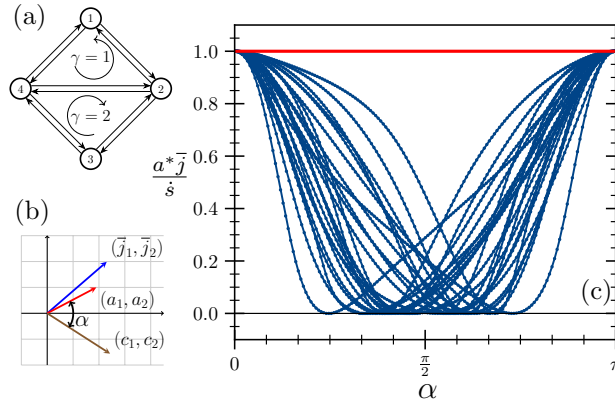


Figure 3: Panel(a): Graph of admissible transitions for the four state model with the two cycles  $\gamma = 1$  and  $\gamma = 2$  as indicated. Panel (b): Sketch of cycle affinities  $(a_1, a_2)$ , cycle currents  $(j_1, j_2)$ , and cycle coefficients  $(c_1, c_2)$  plotted in  $\mathbb{R}^2$ , with the angle  $\alpha$  indicated. Panel (c):  $a^* \bar{j}$  as a function of  $\alpha$  for  $\bar{j} = 1$ . Different lines correspond to different choices of the rates  $\mathbf{q}_{xy}$ , here randomly generated with uniform distribution between 0 and 1.

As an illustration of the applicability of the effective affinity to driven diffusions, we analyse in this section the effective affinity for a particle that is subject to a constant non-conservative force  $f$  and undergoes overdamped diffusion on a ring. We show that in this model the effective affinity of an arbitrary current equals the macroscopic (thermodynamic) affinity. Furthermore, we derive an explicit expression for the martingale  $M_t$ , and we show that  $M_t$  is different from the exponentiated negative entropy production. Lastly, we show that the equality in Eq. (6) is attained. These properties are similar to those of currents in Markov jump processes defined on unicyclic graphs.

### 8.1 Currents in a Brownian particle on a ring

We consider a particle that is bound to a one-dimensional ring and is immersed into an isothermal environment. The evolution in time of the particle's position,  $X_t \in [0, 1)$ , is described by the stochastic differential equation

$$\frac{dX_t}{dt} = \frac{f}{\gamma} + \sqrt{2D} \frac{dW_t}{dt}, \quad (50)$$

where  $f$  is the non-conservative force acting on the particle,  $\gamma$  is the frictional coefficient,  $D$  is the particle's diffusion coefficient, and  $W_t$  is a standard Wiener process representing the stochastic force that the environment exerts on the particle. We assume that the frictional coefficient is related to temperature by Einstein's relation

$$D = \frac{k_B T_{\text{env}}}{\gamma} \quad (51)$$

where  $T_{\text{env}}$  is the temperature.

The probability density function  $p_t(x)$  of the particle's position evolves according to the Fokker-Planck equation

$$\partial_t p_t(x) = \mathcal{L}^\dagger p_t(x), \quad (52)$$

with

$$\mathcal{L}^\dagger = -f \partial_x + D \partial_x^2, \quad (53)$$



and with periodic boundary conditions,  $p_t(x+1) = p_t(x)$ .

For one-dimensional driven diffusions, fluctuating currents  $J_t$  are Stratonovich integrals of the form [22]

$$J_t = \int_0^t c(X_s) \circ dX_s, \quad (54)$$

where  $c(x)$  is a bounded, real-valued function on the interval  $[0, 1)$ . The Stratonovich convention, denoted by  $\circ$ , ensures that  $J_t$  is antisymmetric under the time reversal. In the example of  $c(x) = 1$  it holds that  $J_t$  is the net distance travelled by the particle along the ring.

In what follows, we assume, without loss of generality, that  $f > 0$  and we set  $\int_0^1 c(x) dx = 1$ . In this case, the average current is given by

$$\bar{j} = \frac{f}{\gamma}. \quad (55)$$

## 8.2 Effective affinity

Just as was the case for Markov jump processes, we define the effective affinity as the nonzero root of the logarithmic moment generating function, i.e., through Eq. (20), where  $\lambda_J$  is defined as in Eq. (18) with the averages  $\langle \cdot \rangle$  now over different realisations of the diffusion process Eq. (50).

We show that for an arbitrary current of the form (54), determined by the function  $c(x)$ , the effective affinity takes the form

$$a^* = \frac{f}{k_B T_{\text{env}}}, \quad (56)$$

and hence in this model it equals the macroscopic (thermodynamic) affinity divided by the temperature, and the effective affinity is also the stalling force divided by the temperature.

The tilted operator that governs the evolution of  $\langle \exp(-aJ_t) \rangle$  reads [34]

$$\tilde{\mathcal{L}}(a) = \frac{f}{\gamma} (\partial_x - ac(x)) + D(\partial_x - ac(x))^2, \quad (57)$$

and, as for Markov jump processes, the Perron root of  $\tilde{\mathcal{L}}(a)$  equals  $\lambda_J(a)$ . Hence, to find the effective affinity  $a^*$  we solve the eigenvalue problem

$$\tilde{\mathcal{L}}(a^*)[\phi_{a^*}(x)] = \lambda_J(a^*)\phi_{a^*}(x) = 0 \quad (58)$$

with the periodic boundary condition  $\phi_{a^*}(x+1) = \phi_{a^*}(x)$ . Note that we are solving (58) towards both  $a^*$  and  $\phi_{a^*}$ , the latter being the right eigenvector of  $\tilde{\mathcal{L}}(a)$  with eigenvalue  $\lambda_J(a)$ , and  $a^*$  the value of the parameter  $a$  for which the  $\lambda_J(a)$  vanishes.

Making the transformation [49]

$$\phi_a(x) = \exp\left(a \int_0^x c(y) dy\right) s_a(x), \quad (59)$$

we find that Eq. (58) is equivalent to the differential equation

$$\frac{f}{\gamma} \partial_x s_{a^*}(x) + D \partial_x^2 s_{a^*}(x) = 0, \quad (60)$$

which is subject to the boundary condition

$$s_{a^*}(x+1) = s_{a^*}(x) \exp\left(-a^* \int_0^1 c(y) dy\right) = e^{-a^*} s_{a^*}(x), \quad (61)$$

and we have used here that  $\int_0^1 c(y)dy = 1$ . The equation (60) admits the general solution

$$s_{a^*}(x) = \zeta_1 \frac{D\gamma}{f} \exp\left(-\frac{f}{D\gamma}x\right) + \zeta_2. \quad (62)$$

To satisfy the boundary conditions (61), we set  $\zeta_1 = 1$  and  $\zeta_2 = 0$ , yielding

$$s_{a^*}(x) = \frac{D\gamma}{f} \exp\left(-\frac{f}{D\gamma}x\right). \quad (63)$$

Substituting Eq. (63) into (61), and using Einstein's relation (51), we find the result Eq. (56) for the effective affinity that we were meant to derive.

### 8.3 Martingale

In this example, the martingale Eq. (27) reads

$$M_t = \frac{k_B T_{\text{env}}}{f} \exp\left(-\frac{f}{k_B T_{\text{env}}} \left( \int_0^t c(X_s) \circ dX_s - \int_0^{X_t} (c(y) - 1) dy \right)\right), \quad (64)$$

where the second term  $-\int_0^{X_t} (c(y) - 1) dy$  is a contribution from the right eigenvector  $\phi_{a^*}(X_t)$ ; notice that the second term is not time extensive as  $\int_0^1 c(x) dx = 1$ . In the specific case when  $c = 1$ , we get

$$M_t = \frac{k_B T_{\text{env}}}{f} \exp\left(-\frac{f}{k_B T_{\text{env}}} X_t\right) = \frac{k_B T_{\text{env}}}{f} \exp(-S_t), \quad (65)$$

with  $S_t = -fX_t/(k_B T_{\text{env}})$  is the stochastic entropy production [22], and we thus recover the martingale of Ref. [50].

### 8.4 Dissipation bound: all currents are optimal

We show that for all currents  $J$  the equality in Eq. (6) is attained, and hence all currents are optimal.

Indeed, since the rate of dissipation equals (see e.g., Chapter 5 of Ref. [39])

$$\dot{s} = \frac{f^2}{\gamma k_B T_{\text{env}}}, \quad (66)$$

it follows from Eqs. (56), (55), and (66) that

$$a^* \bar{j} = \dot{s}, \quad (67)$$

and therefore the equality in (6) is attained.

The optimality of currents in the present model can also be understood from an application of cycle equivalence classes to a discretised version of the model. Indeed, since the discretised model is unicyclic, the graph of admissible transitions has one fundamental cycle, and hence all currents belong to the same cycle equivalence class (up to a constant). Note that since this result follows from the topology of the underlying graph of admissible transitions, the equalities in Eqs. (6) and (42) are also attained when a space dependent force is added to the present model.

## 9 Effective affinity and stalling forces in a Kinesin-1 model

So far, we have shown that the effective affinity is closely related to the dissipation of a current and to its fluctuations. Nevertheless, the question remains whether we can give a mechanical interpretation to the effective affinity, in the sense of a generalised force. Since the current,  $\bar{j}$ , vanishes when the effective affinity equals zero,  $a^*$  cannot represent the thermodynamic force acting on the system, yet it may still be the current's stalling force. In this section, we make a study of the potential connection between the effective affinity and stalling forces.

First in Sec. 9.1 we review results for stalling forces from Ref. [18], where the problem was solved for edge currents. Next, in Sec. 9.2 we consider a case study on a biophysical model for Kinesin-1 for which the positional current is not an edge current, and thus the generic effective affinity studied in this paper is relevant. In Sec. 9.3 we show that in this biophysical model the effective affinity is approximately equal to the stalling force, and we show that this property is lost when a set of thermodynamic consistency conditions are violated. These findings suggest that effective affinities and stalling forces are related, but delineating the precise relationship between these two quantities beyond the present toy model remains an open problem.

### 9.1 Stalling forces

Markov processes modelling physical systems often depend on external parameters such as chemical potentials or physical forces, which modify the rates of the Markov process. An interesting property of the edge current effective affinity (23) is that it has a physical interpretation in terms of these external parameters.

Let the current of interest be  $J_t^{xy}$ , i.e., the net number of jumps along the edge  $(x, y)$ , and let us assume that a physical force  $f$  acts on the system through the  $(x, y)$  edge by modifying the rates  $\mathbf{q}_{xy}$  and  $\mathbf{q}_{yx}$ . An example of such a conjugate current-force pair is discussed in Refs. [19, 51] where  $J_t^{xy}$  is the positional current of a molecular motor and  $f$  is the mechanical force acting on the motor. Using the principle of local detailed balance [7, 8], we can express the ratio of the rates by

$$\frac{\mathbf{q}_{xy}}{\mathbf{q}_{yx}} = \frac{\mathbf{q}_{xy}^{(0)}}{\mathbf{q}_{yx}^{(0)}} \exp\left(-\frac{fd}{k_B T_{\text{env}}}\right), \quad (68)$$

where the minus sign indicates that the force opposes the positive direction of flow in the definition of  $J_t^{xy}$ , where  $T_{\text{env}}$  is the temperature,  $k_B$  is the Boltzmann constant, and where  $d$  is the distance crossed by the system when  $X$  jumps from  $x$  to  $y$ . The matrix  $\mathbf{q}^{(0)}$  denotes the transition rates when the force  $f = 0$ .

As shown in Ref. [23], the effective affinity equals the *additional* force required to stall the current (i.e, to ensure  $\bar{j}^{-xy} = 0$ ), which we call the stalling force. Hence, the effective affinity takes the form

$$a^* = \frac{(f_0 - f)d}{k_B T_{\text{env}}} =: f_{\text{stall}}, \quad (69)$$

where  $f_0$  is the stalling force when  $f = 0$  and  $f - f_0$  is the stalling force for nonzero  $f$ . Notice that for convenience we introduce the symbol  $f_{\text{stall}}$  for the dimensionless form of the stalling force.

For edge currents,  $f_0$  is defined by the condition that for  $f = f_0$  it holds that

$$r_{ss}(x)\mathbf{r}_{xy} - r_{ss}(y)\mathbf{r}_{yx} = 0, \quad (70)$$

where  $\mathbf{r}$  is the matrix of transition rates

$$\mathbf{r}_{x'y'} = \begin{cases} \mathbf{q}_{x'y'}^{(0)} & \text{if } (x'y') \neq (xy), \\ \mathbf{q}_{xy}^{(0)} \exp\left(-\frac{f_0 d}{k_B T_{\text{env}}}\right) & \text{if } (x'y') = (xy), \end{cases} \quad (71)$$

and where  $r_{ss}$  is the stationary probability mass function of the Markov process with rate matrix  $\mathbf{r}$ .

In the next section, we verify whether (69) still holds in a biophysical model of Kinesin-1 for which the positional current is not an edge current.

## 9.2 Biophysical model for Kinesin-1

We define a biochemical model for the motor protein Kinesin-1 [52] that we use to study effective affinities and stalling forces in motor proteins. Kinesin-1 proteins are motor proteins that bind to quasi one-dimensional biofilaments. Once they are bound to their substrate, the Kinesin-1 motors perform directed motion towards the biofilament's plus end. This directed motion is fueled by a hydrolysis reaction that converts adenosine triphosphate (ATP) into adenosine diphosphate and an inorganic phosphate molecule. The free energy released in this reaction is converted into work that generates the directed runs. Hence, the entropy production takes the form

$$\dot{s} = \frac{\Delta\mu}{k_B T_{\text{env}}} \bar{j}_{[\text{ATP}]} - \frac{fd}{k_B T_{\text{env}}} \bar{j}_{\text{pos}}, \quad (72)$$

where  $\Delta\mu$  is the chemical potential difference between the products and the reactants of the hydrolysis reaction,  $f$  is the mechanical force opposing the motion of kinesin-1 towards the microtubule plus end,  $d$  is the distance covered in one motor step,  $T_{\text{env}}$  is the temperature of the environment, and  $k_B$  is the Boltzmann constant (as before). The currents  $\bar{j}_{[\text{ATP}]}$  and  $\bar{j}_{\text{pos}}$  count, respectively, the number of ATP molecules hydrolysed and the number steps made by the motor in a unit of time.

Next, we consider a Markov jump process that provides a microscopic model for the dynamics of Kinesin-1 motors, viz., we consider the model of Ref. [52]. This biophysical model of Kinesin-1 consists of five states, each corresponding to specific chemical and physical configurations of the two motor heads of Kinesin-1. In each of these states, each head of the motor can either be attached or detached from the microtubule, and also be in any one of ATP, or ADP·Pi binding state or be unbound. The graph of admissible transitions of this model is shown in Fig. 4(a), and as indicated therein, can be decomposed into three fundamental cycles. The two ‘‘forward’’ cycles indicated in Fig. 4(a) correspond to a series of transitions in which the motor takes one full step forward. The other cycle represents a series of transitions where the motor does not move forward, and is hence labeled ‘‘futile’’. Furthermore, each step of the motor consists of two substeps, corresponding to the attachment of the head closer to the plus end of the microtubule (the forward head) and the detachment of the head further away (the rear head). This is consistent with experimental data [53, 54]. The distinction between the two ‘‘forward’’ cycles is chiefly that in cycle 1231 the rear head of the motor detaches from the microtubule before ATP is bound to the forward head, while in cycle 2342 the ATP binding on the forward head occurs before the rear head detaches from the microtubule, thus representing distinct pathways for forward stepping. A detailed explanation of all the states and the transitions in the model may be found in Fig.1 of [52]. The positional current  $J_{\text{pos}}$ , which gives the displacement of the molecular motor, sums up contributions the edges (1, 3), (4, 2) and (2, 3), accounting for both the ‘‘forward’’ cycles (see Appendix D for details).

We discuss the dependency of the rates  $\mathbf{q}_{xy}$  in the model on the two external parameters, namely, the concentration of ATP in the environment (that regulates the chemical potential difference  $\Delta\mu$  and is denoted by  $[\text{ATP}]$ ), and the mechanical force  $f$  experienced by the motor. The transitions  $3 \rightarrow 4$  and  $1 \rightarrow 2$  represent the binding of ATP to one of the motor heads, and therefore

$$\mathbf{q}_{34} = \mathbf{q}_{12} = \mathbf{q}_{12}^0 [\text{ATP}], \quad (73)$$

where  $\mathbf{q}_{12}^0$  is a constant. The transitions  $4 \rightleftharpoons 2, 2 \rightleftharpoons 3$  and  $3 \rightleftharpoons 1$  all correspond to the

detachment or attachment of one of the heads of the molecular motor from the microtubule, which is the “stepping” of the motor. These transitions are thus affected by the mechanical force  $f$  which modifies their rates according to

$$\mathbf{q}_{xy} = \mathbf{q}_{xy}^0 \exp\left(-\delta_{xy} \frac{fd}{k_B T_{\text{env}}}\right) \quad (74)$$

for transitions corresponding to forward steps and

$$\mathbf{q}_{xy} = \mathbf{q}_{xy}^0 \exp\left(\delta_{xy} \frac{fd}{k_B T_{\text{env}}}\right) \quad (75)$$

for transitions corresponding to backward steps. Here the force distribution factors  $\delta_{xy}$  are non-negative real parameters that determine the extent to which the transition from  $x$  to  $y$  is affected by the mechanical force  $f$ . In our simulations we use the values of the load distribution factors and the transition rates from Ref. [52] that obtained these parameters from fits to experimental data; we specify all parameters used in Appendix D.

We now fix the coefficients  $c_{xy}$  defining the positional current  $J_{\text{pos}}$ . Each step of the motor, of length  $d$ , consists of two substeps both forward stepping cycles. Since the total step size in both cycles is the same, we get the equality

$$c_{23} + c_{21} = c_{23} + c_{42} = 1, \quad (76)$$

where we have normalized the coefficients such that the current  $J_{\text{pos}}$  is non-dimensionalized. Next, we use thermodynamic consistency to relate the coefficients  $c_{xy}$  to the force distribution factors  $\delta_{xy}$ . On one hand, the entropy produced in the environment when the motor moves from state  $x$  to state  $y$  equals

$$\frac{f}{k_B T_{\text{env}}} c_{xy} d. \quad (77)$$

On the other hand, due to local detailed balance the entropy change in the environment is given by

$$\ln \frac{\mathbf{q}_{xy}}{\mathbf{q}_{yx}} = \frac{fd}{k_B T_{\text{env}}} (\delta_{xy} + \delta_{yx}). \quad (78)$$

Equating (77) with (78) yields the thermodynamic consistency condition

$$c_{xy} = \delta_{xy} + \delta_{yx} \quad (79)$$

that relates the current coefficients to the force distribution factors.

### 9.3 Effective affinity equals the stalling force

We now address the question of whether the effective affinity in the present model is a stalling force, i.e., whether Eq. (69) applies in this model. In Fig 4(b), we plot  $a^*$  as a function of  $f$  and compare it with a plot of Eq (69). Remarkably, the two appear to correspond well. However, upon closer examination we find a systematic deviation from the linear behaviour of Eq. (69). The systematic deviation is clear from Fig. 5(a) that shows the difference between the effective affinity  $a^*$  and the dimensionless form of the stalling force  $f_{\text{stall}}$  as a function of  $f$ . The difference  $a^* - f_{\text{stall}}$  is a bounded function that saturates for large values of  $f$ , and is small compared to  $a^*$  (the ratio  $1 - f_{\text{stall}}/a^* \approx 1e - 3$  except near stalling when  $a^* \approx 0$ , see Fig. 5(b)), and the absolute difference. Hence, although the effective affinity is not equal to the stalling force, we nevertheless find that in this model the stalling force closely approximates the effective affinity.

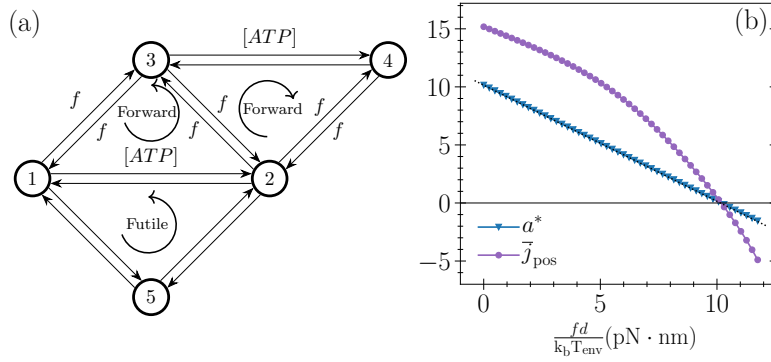


Figure 4: Panel (a): Graph of admissible transitions in the mechanochemical model of Kinesin-1 from Ref. [52]. The model has three cycles, two corresponding with forward motion and one futile cycle. The dependence of the rates on the mechanical forces  $f$  and  $[ATP]$  are as indicated. See Appendix B.1 for the model parameter values. (b) The average positional current  $\bar{j}$  (purple circles) and effective affinity  $a^*$  (blue triangles) as a function of  $f$ . The effective affinity  $a^*$  is obtained by numerically diagonalising  $\tilde{\mathbf{q}}(a)$  and numerically finding the value of  $a$  for which the largest eigenvalue equals zero. The markers for  $\bar{j}$  are obtained by numerically calculating the steady state of the Markov process through a linear solver. The black dashed line shows Eq. (69) for this model.

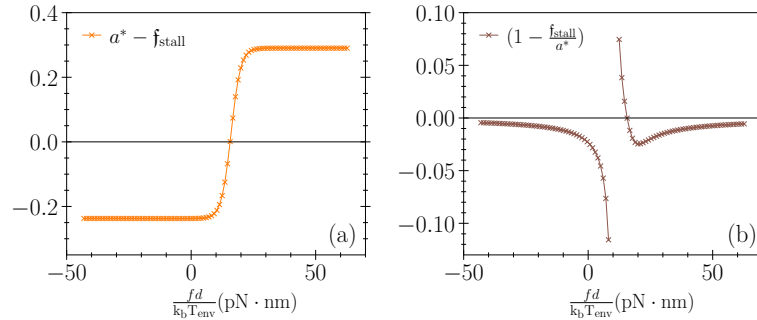


Figure 5: *Difference between the effective affinity  $a^*$  and the stalling force* — The left panel (a) shows the difference between the left and right hand sides of Eq (69), hence the difference between the effective affinity, and its estimated value based on the stalling force, is a bounded function over a large range of  $f$ . Further, the difference is small compared to the value of  $a^*$ . The right panel (b) shows same quantity, now divided by  $a^*$  to show the relative scale of the difference. In the plot on the right, three data points in the center have been excluded to avoid the points where  $a^*$  is very close to zero and thus the relative error diverges.

The numerical observation that the effective affinity is almost equal to the stalling force, is closely related to the fact that the model is thermodynamically consistent, in the sense that Eq. (79) holds. Indeed, if we modify the model such that Eq. (79) is not anymore valid, then the effective affinity deviates significantly from the stalling force (see Appendix E). In addition, the approximate linear scaling of  $a^*$  with  $f$  with slope  $-1$  is clearly violated for models for which the thermodynamic consistency condition (79) does not hold (results not shown).

## 10 Discussion

We have introduced effective affinities for generic currents in stationary Markov processes. The effective affinity is a (unique) real number associated with a fluctuating current that quantifies several physical properties. Notably, the effective affinity multiplied by the average current lower bounds dissipation, as expressed by the inequality (6), and the effective affinity is the exponential decay constant that characterises the tails of the infimum statistics of the current, as stated in Eq. (8). Furthermore, we have shown that all fluctuating currents that are cycle equivalent with  $kS_t$ , with  $k$  a constant, are optimal in the sense that for those currents the equality in (6) is attained.

From a methodological point of view, this paper introduces a new class of martingales  $M_t$ , given by Eq. (27), that are associated with generic currents. The martingale  $M_t$  is an exponential martingale, and the prefactor that appears in the exponential in front of the current is the negative effective affinity. Martingales considered before in the literature, such as the exponentiated negative entropy production [24–26] and the exponential martingale for edge currents derived in Ref. [19], are special cases of the martingale  $M_t$ . Given the numerous properties of martingales, as outlined in [39], the exponential martingale  $M_t$  adds to existing techniques for studying current fluctuations. Notably, in this Paper we have used  $M_t$  to derive the thermodynamic trade off relation Eq. (42) that expresses an inequality between speed (quantified by  $\langle T \rangle$ ), uncertainty (quantified by  $p_-$ ), and dissipation (quantified by  $\dot{s}$ ). The derivation in this paper based on martingales is different from the one in Ref. [27], and the present derivation is arguably more clear as it does not rely on a scaling argument. Another interesting aspect of the martingales  $M_t$  is that they relate large deviation theory (as  $a^*$  is the nonzero root of the equation  $\lambda_J(a) = 0$ ) with the extreme value statistics of the current (as  $a^*$  is the exponential decay constant in the tails of the infimum statistics of  $J$ ).

For edge currents, the effective affinity  $a^*$  equals the effective affinity for edge currents, as studied in Refs. [18, 23]. We have shown that several properties of the edge effective affinity generalise to the effective affinity defined in this paper. However, there are a few properties that we have not explored in this Paper. Notably, Ref. [55, 56] derives a detailed fluctuation relation for currents, which holds as long as the distribution is evaluated at the random time when a fixed number of transitions have been observed, and Ref. [57] shows that the effective affinity determines the Kullback-Leibler divergence due to subsequent transitions along an edge. How these properties extend to the case of generic currents remains an open problem.

The last three sections (Secs. 7, 8, and 9) are case studies for three important problems. We discuss here how these problems can be generalised.

An interesting open problem is to identify the fluctuating currents that are optimal, in the sense that for these currents the equality in (42) is attained. We know that the set of optimal currents contains the sets  $[kS_t]$  of currents that are cycle equivalent with the stochastic entropy production  $S_t$ , up to a proportionality constant  $k$ . However, it remains open whether there exist currents that are optimal even though they are not in one of the sets  $[kS_t]$ . Numerical analysis in simple models, such as the Markov jump process in Sec. 7, indicate that all optimal currents are contained in the sets  $[kS_t]$ . However, we do not have a mathematical argument to support this numerical observation, and therefore this interesting question remains open.

Although we have focused in this paper on time-homogeneous Markov processes defined on a discrete set, the definition of the effective affinity as the nonzero root of  $\lambda_J(a) = 0$  also applies to overdamped Langevin processes. To verify this claim, we have analysed in Sec. 8 the effective affinity in a Brownian particle bound on a ring that is subject to a constant external force. We have shown that for any current in this model the effective affinity is the thermodynamic force acting on the current, and therefore all currents are optimal. We have also derived an explicit expression for the martingale  $M_t$  of a generic fluctuating current. Extending the

present theory to generic overdamped Langevin processes requires us to extend the formalism of the present paper to this setup, and will be considered in future work. At present, is not entirely clear how to extend the definition of cycle equivalence classes to Langevin processes; the framework of Refs. [58, 59] that defines cycle currents in Langevin processes as 2-forms may be useful to this purpose.

This brings us to the last case study, which investigates the relationship between the effective affinity and the stalling force. Since the effective affinity equals zero when the current is zero, it can in general not be identified with the thermodynamic force (except for unicyclic systems, such as a Brownian particle bound on a ring), but there may still be a connection with the stalling force. In Sec. 9, we have numerically analysed the effective affinity and stalling force of a biophysical model of Kinesin-1. If this model is thermodynamically consistent, then the effective affinity and the stalling force are approximately equal (the relative difference  $1 - f_{\text{stall}}/a^* \approx 1e - 3$ ). On the other hand, if the thermodynamic consistency condition (79) is violated, then we have observed a significant difference between the effective affinity  $a^*$  and the stalling force  $f_{\text{stall}}$ . Hence, for this biophysical model we can conclude that for practical purposes the stalling force can be used to estimate the effective affinity. This observation is interesting as it relates via Eq. (8) the exponential decay constant of the infima of the positional current of Kinesin-1 motors to the stalling force. In addition, the stalling force can be used to estimate the rate of dissipation through  $f_{\text{stall}}\bar{j}$ . It remains to be understood whether the close relationship between the effective affinity and the stalling force is a specific property of this model, or whether it is generally applicable to thermodynamically consistent models.

## Acknowledgments

We thank Nikolas Nüsken for discussions and guidance, we thank Stefano Bo for a detailed reading of the manuscript, and we thank Friedrich Hübner, Gabriele Pinna, Christian Maes, Anupam Kundu, and Alvaro Lanza Serrano for fruitful discussions.

## A Model parameters for Figure 1

Figure 1 shows  $\lambda_J$  and  $\lambda_{S'}$  for the Markov jump model with a graph of admissible transitions as illustrated in Figure 2. The transition rates between the states are set equal to  $\mathbf{q}_{12} = 3$ ,  $\mathbf{q}_{41} = 3$ ,  $\mathbf{q}_{21} = 1$ ,  $\mathbf{q}_{14} = 1$ ,  $\mathbf{q}_{23} = 2$ ,  $\mathbf{q}_{34} = 2$ ,  $\mathbf{q}_{32} = 1$ ,  $\mathbf{q}_{43} = 1$ ,  $\mathbf{q}_{24} = 3$ , and  $\mathbf{q}_{42} = 1$ , and the current  $J$  current is defined by the coefficients  $c_{12} = -c_{21} = 1.26913$ ,  $c_{34} = -c_{43} = 1.37403$ , and all other  $c_{x,y}$  coefficients are set to 0. For the abovementioned rates the entropy production rate  $\dot{s} = 1.94745$ ; notice that in the figure this is equal to the nonzero root of  $\lambda_{S'}$ . The curves for  $\lambda_J$  and  $\lambda_{S'}$  are obtained by numerically diagonalising the corresponding matrix  $\tilde{\mathbf{q}}$ . The current  $S'$  is the current with coefficients  $c_{xy} = \frac{1}{\dot{s}} \ln\left(\frac{\mathbf{q}_{xy}}{\mathbf{q}_{yx}}\right)$ .

## B Effective affinity for edge currents

Here we consider the limiting case of edge currents  $J_t = J_t^{xy}$  that count the net number of jumps along an edge  $(x, y)$  of the graph of admissible transitions of the Markov chain  $X$ . In Sec. B.1 we show that the effective affinity for edge currents takes the form given in Eq. (23), and in Sec. B.2 we show that the Martingale  $M_t$ , as defined in Eq. (27), is equivalent to the



martingale in Eq. (69) of Ref. [19].

### B.1 Effective affinity for edge currents

We show that for edge currents the effective affinity is given by

$$a^* = \ln \frac{p_{ss}^{(x,y)}(x) \mathbf{q}_{xy}}{p_{ss}^{(x,y)}(y) \mathbf{q}_{yx}}, \quad (\text{B.1})$$

where the right-hand side of (B.1) is the Poletti-Esposito affinity defined in Refs. [16, 18, 19], and the left-hand side is the effective affinity as defined in Eq. (20).

In Eq. (B.1), the  $p_{ss}^{(x,y)}$  is the stationary distribution of a Markov jump process with the  $\mathbf{q}$ -matrix  $\mathbf{q}^{(x,y)}$  that has off-diagonal entries given by

$$\mathbf{q}_{rs}^{(x,y)} = \begin{cases} 0, & (r,s) \in \{(x,y), (y,x)\}, \\ \mathbf{q}_{rs}, & (r,s) \in \mathcal{X}^2 \setminus (\{(x,y), (y,x)\} \cup \{(z,z) : z \in \mathcal{X}\}), \end{cases} \quad (\text{B.2})$$

and diagonal entries given by

$$\mathbf{q}_{rr}^{(x,y)} = - \sum_{z \in \mathcal{X} \setminus \{r\}} \mathbf{q}_{rz}^{(x,y)}. \quad (\text{B.3})$$

We assume this Markov process is ergodic, which implies that  $p_{ss}^{(x,y)}$  is a strictly positive eigenvector of  $\mathbf{q}^{(x,y)}$  with eigenvalue zero.

By definition, the effective affinity  $a^*$  is the value of  $a$  at which the Perron root of  $\tilde{\mathbf{q}}(a)$  equals zero. In the present example of an edge current, the tilted matrix  $\tilde{\mathbf{q}}(a)$  is given by Eq. (25) with  $c_{xy} = -c_{yx} = 1$  and all other  $c$ -coefficients equal to 0, leading to the expression

$$\tilde{\mathbf{q}}_{rs}(a) = \begin{cases} \mathbf{q}_{xy} e^{-a}, & (r,s) = (x,y), \\ \mathbf{q}_{yx} e^a, & (r,s) = (y,x), \\ \mathbf{q}_{rs}, & (r,s) \in \mathcal{X}^2 \setminus (\{(x,y), (y,x)\} \cup \{(z,z) : z \in \mathcal{X}\}), \\ -\sum_{z \in \mathcal{X} \setminus \{r\}} \mathbf{q}_{rz}, & r = s. \end{cases} \quad (\text{B.4})$$

To derive Eq. (B.1), we need to show that if  $a$  takes the value in the right-hand side of Eq. (B.1), then the Perron root of the matrix  $\tilde{\mathbf{q}}(a)$  vanishes. This latter follows from the fact that: (i) when  $a$  equals the right-hand side of Eq. (B.1), then  $p_{ss}^{(x,y)}$  is a left eigenvector of  $\tilde{\mathbf{q}}(a)$  with eigenvalue zero; (ii) any strictly positive left eigenvector of a positive matrix is a left eigenvector of its Perron root, see Theorem 1.4 of Ref. [60].

In what follows, we show that if  $a$  equals the right-hand side of Eq. (B.1), then  $p_{ss}^{(x,y)}$  is a left eigenvector of  $\tilde{\mathbf{q}}(a)$  with zero eigenvalue, i.e., we demonstrate that

$$\sum_{s \in \mathcal{X} \setminus \{r\}} \tilde{\mathbf{q}}_{sr}(a) p_{ss}^{(x,y)}(s) - \tilde{\mathbf{q}}_{rr}(a) p_{ss}^{(x,y)}(r) = 0, \quad \forall r \in \mathcal{X} \quad (\text{B.5})$$

holds for the corresponding value of  $a$ .

For  $r \in \mathcal{X} \setminus \{x, y\}$  Eq. (B.5) is identical to

$$\sum_{s \in \mathcal{X} \setminus \{x\}} \mathbf{q}_{sr} p_{ss}^{(x,y)}(s) - \mathbf{q}_{rr} p_{ss}^{(x,y)}(r) = 0, \quad (\text{B.6})$$

which we recognise as the stationary condition that defines  $p_{ss}^{(x,y)}$ , and is thus satisfied. For  $r = x$ , Eq. (B.5) is identical to

$$\sum_{s \in \mathcal{X} \setminus \{x\}} \tilde{\mathbf{q}}_{sx}(a) p_{ss}^{(x,y)}(s) - \tilde{\mathbf{q}}_{xx}(a) p_{ss}^{(x,y)}(x) = 0 \quad (\text{B.7})$$

$$\Leftrightarrow \mathbf{q}_{yx} e^a p_{ss}^{(x,y)}(y) - \mathbf{q}_{xy} p_{ss}^{(x,y)}(x) = 0 \quad (\text{B.8})$$

$$\Leftrightarrow a = \ln \frac{p_{ss}^{(x,y)}(x) \mathbf{q}_{xy}}{p_{ss}^{(x,y)}(y) \mathbf{q}_{yx}}, \quad (\text{B.9})$$

which yields the assumed value of  $a$ . Equation (B.8) follows from (B.7), (B.4), and (B.6) for  $r = x$ . Analogously one can show that Eq. (B.5) holds for  $r = y$ .

## B.2 Martingale for edge currents

We show that for edge currents the martingale  $M_t$  from Eq. (27) is equivalent with the martingale

$$M_t^{xy} := \frac{p_{ss}^{(x,y)}(X_0) q_{ss}(X_t)}{p_{ss}^{(x,y)}(X_t) p_{ss}(X_0)} \exp(-a^* J_t^{xy}), \quad (\text{B.10})$$

defined in Ref. [19], in the sense that the two martingales are equal up to a prefactor that is constant in time. Note that the prefactor is nevertheless random as it depends on the initial state  $X_0$ . In Eq. (B.10)  $q_{ss}$  is the steady state of the modified Markov process with rate matrix

$$\mathbf{l}_{uv} = \begin{cases} \mathbf{q}_{uv}, & \text{for } (u, v) \in \{(x, y), (y, x)\}, \\ \frac{p_{ss}^{(x,y)}(v)}{p_{ss}^{(x,y)}(u)} \mathbf{q}_{vu}, & \text{for } (u, v) \in \mathcal{X}^2 \setminus \{(x, y), (y, x)\}. \end{cases} \quad (\text{B.11})$$

As we show in this appendix,

$$\phi_{a^*}(z) = \frac{q_{ss}(z)}{p_{ss}^{(x,y)}(z)}, \quad (\text{B.12})$$

for all  $z \in \mathcal{X}$ , and therefore it holds that

$$M_t^{xy} = \frac{p_{ss}^{(x,y)}(X_0)}{p_{ss}(X_0)} M_t, \quad (\text{B.13})$$

and the two martingales are equivalent.

Equation (B.12) follows from the fact that

$$\phi_{a^*}(z) = p_{ss}^{(x,y)}(z) \quad (\text{B.14})$$

and

$$q_{ss}(z) = (p_{ss}^{(x,y)}(z))^2, \quad (\text{B.15})$$

for all  $z \in \mathcal{X}$ .

We derive Eq. (B.14) by noticing that  $\mathbf{l}$  can be expressed as

$$\mathbf{l} = \mathbf{p}_{ss}^{-1(x,y)} \tilde{\mathbf{q}}(a^*) \mathbf{p}_{ss}^{(x,y)}, \quad (\text{B.16})$$

where  $\mathbf{p}_{ss}^{(x,y)}$  is a diagonal matrix with diagonal entries given by  $p_{ss}^{(x,y)}(z)$ , and  $\mathbf{p}_{ss}^{-1(x,y)}$  is its inverse. In addition, it holds that

$$\phi_{a^*}^{-1} \tilde{\mathbf{q}}(a^*) \phi_{a^*} \quad (\text{B.17})$$

is a Markov matrix, as it is a special case of the generalized Doob transform [34]

$$\phi_a^{-1} \tilde{\mathbf{q}}(a) \phi_a - \lambda(a) \mathbb{1}. \quad (\text{B.18})$$

Note that we used again the symbol  $\phi_a$  for a diagonal matrix with diagonal entries given by the right eigenvector  $\phi_a(z)$  of  $\tilde{\mathbf{q}}(a)$ , and  $\mathbb{1}$  is the identity matrix. Equation (B.14) follows from that fact that Eqs. (B.16) and (B.17) are both Markov matrices, and therefore the diagonal transformations in the two equations are identical up to a constant normalisation factor, which we can set to one.

Furthermore, left multiplying Eq. (B.16) by the vector with entries  $(p_{ss}^{(x,y)}(z))^2$ , and using that  $p_{ss}^{(x,y)}(z)$  is the left eigenvector of  $\tilde{\mathbf{q}}(a^*)$ , as shown in Sec. B.1, we find that the vector with entries  $(p_{ss}^{(x,y)}(z))^2$  is the left null eigenvector of the matrix  $\mathbf{I}$ , and therefore equals  $q_{ss}$  as stated in Eq. (B.15).

## C Currents in the same cycle equivalence classes have the same effective affinity

In this appendix we derive Eq. (49) that expresses the characteristic polynomial of the matrix  $\tilde{\mathbf{q}}(a)$  as a sum over spanning, linear subgraphs of the graph of admissible transitions of the Markov chain  $X$ .

The appendix is structured as follows. First, in Sec. C.1 we define fundamental cycle basis  $\mathcal{C}$  of a graph, which we use in Sec. 6.1 to define the cycle coefficients  $c_\gamma$  and the cycle equivalence classes  $[J_t]$ . In the following three sections, we derive the expression Eq. (49). First, in Sec. C.2, we use the Coefficients Theorem for directed graphs to express the characteristic polynomial of  $\tilde{\mathbf{q}}(a)$  as a sum over linear subgraphs. Second, in Sec. C.3 we define the coefficients  $c_{\mathcal{C}}$  associated with directed cycles  $\mathcal{C}$ , and we show that these coefficients can be expressed as a linear combination of the cycle coefficients  $c_\gamma$ . Lastly, in Sec. C.4 we combine the above arguments to obtain Eq. (49).

### C.1 Fundamental cycle basis

We construct a set of cycles  $\mathcal{C}$ , known as a fundamental cycle basis, associated with a nondirected graph  $\mathcal{G} = (\mathcal{X}, \mathcal{E})$ , where  $\mathcal{X}$  is the set of vertices and  $\mathcal{E}$  the set of nondirected edges. A cycle is an ordered sequence  $\gamma = [x_1, x_2, \dots, x_{n(\gamma)}, x_1]$  of nodes  $x_i \in \mathcal{X}$  such that  $(x_i, x_{i+1}) \in \mathcal{E}$  for all  $i$  and each vertex is only traversed once; notice that reversing the sequence leaves the cycle invariant. A cycle basis is a minimal set of cycles, called basis cycles, such that any cycle  $\gamma$  of  $\mathcal{G}$  can be expressed as a symmetric difference of basis cycles. The set  $\mathcal{C}$ , known as a fundamental cycle basis of the graph  $\mathcal{G}$  is a cycle basis that can be constructed from a spanning tree  $\mathcal{T}$  of  $\mathcal{G}$ . The spanning tree  $\mathcal{T}$  has a number  $|\mathcal{X}| - 1$  of edges, and hence there are a number  $|\mathcal{E}| - |\mathcal{X}| + 1$  of edges in  $\mathcal{E}$  that do not belong to the spanning tree. Adding one new edge to a spanning tree creates a graph with one cycle, and in this way we can define a number  $|\mathcal{E}| - |\mathcal{X}| + 1$  of cycles  $\gamma \in \mathcal{C}$ , and the set  $\mathcal{C}$  forms a basis of the cycle space, which we refer to as a fundamental cycle basis. See also Ref. [47, 61] for more detailed definitions.

In Sec. 6.1 we use a fundamental cycle basis  $\mathcal{C}$  of the graph of admissible transitions of a Markov Jump process to define the coefficients  $c_\gamma$  associated with the basis cycles  $\gamma \in \mathcal{C}$  as

$$c_\gamma := \sum_{i=1}^{n(\gamma)} c_{x_i x_{i+1}}, \quad \gamma \in \mathcal{C}, \quad (\text{C.1})$$

where  $n(\gamma)$  is the number of nodes in  $\gamma$ . We arbitrarily fix a direction in which to perform this sum for each  $\gamma$ , since reversing the order of nodes in a basis cycle  $\gamma$  does not alter the cycle, but would change the sign of  $c_\gamma$  as  $c_{xy} = -c_{yx}$ .

## C.2 Coefficients Theorem applied to $\tilde{\mathbf{q}}(a)$

We now apply the Coefficients Theorem for directed graphs, see Refs. [48, 62], to the matrix  $(\tilde{\mathbf{q}}(a) - \xi \mathbb{1})$ , where  $\mathbb{1}$  is the identity matrix of size  $\mathcal{X}$ . The Coefficients Theorem gives an expression for the determinant of the adjacency matrix of a weighted graph in terms of its spanning linear subgraphs. To apply this theorem, we interpret the matrix  $(\tilde{\mathbf{q}}(a) - \xi \mathbb{1})$  as the adjacency matrix of a weighted directed graph for which  $\mathcal{X}$  is the set of nodes and the nonzero entries of  $(\tilde{\mathbf{q}}(a) - \xi \mathbb{1})$  determine the weights of the directed edges in the graph. Thus, we obtain a graph as illustrated for an example in Panel (a) of Fig. 2.

Using the Coefficients Theorem for a weighted graphs, see Refs. [48, 62] for a detailed description, we express the characteristic polynomial of  $\tilde{\mathbf{q}}(a)$  as

$$\det(\tilde{\mathbf{q}}(a) - \xi \mathbb{1}) = (-1)^{|\mathcal{X}|} \sum_{\mathcal{L} \in \mathcal{L}} (-1)^{\kappa(\mathcal{L})} \prod_{(x \rightarrow y) \in \mathcal{L}} (\tilde{\mathbf{q}} - \xi \mathbb{1})_{yx}, \quad (\text{C.2})$$

where  $\sum_{\mathcal{L} \in \mathcal{L}}$  is a sum over the set  $\mathcal{L}$  of all spanning linear subgraphs  $\mathcal{L}$  of the graph represented by  $(\tilde{\mathbf{q}}(a) - \xi \mathbb{1})$ , and  $\prod_{(x \rightarrow y) \in \mathcal{L}}$  is a product over all directed edges  $(x \rightarrow y)$  that are part of  $\mathcal{L}$  (notice that by our choice of convention, the weight associated with the edge going from node  $x$  to node  $y$  is the entry in the  $y$ -th row and  $x$ -th column of the matrix  $(\tilde{\mathbf{q}}(a) - \xi \mathbb{1})$ ), and where  $\kappa(\mathcal{L})$  is the number of connected components in  $\mathcal{L}$ .

A *linear subgraph* is a subgraph for which the indegree and outdegree of all nodes equals 1. Thus,  $\mathcal{L}$  is the disjoint union of linear directed cycles, which we differentiate into the following three types:

1. cycles consisting of one edge, i.e.,  $(x \rightarrow x) \in \mathbb{S}_{\mathcal{L}}$  (self loops);
2. cycles consisting of two directed edges, i.e.,  $\{(x \rightarrow y), (y \rightarrow x)\} \in \mathbb{E}_{\mathcal{L}}$ ;
3. cycles that have three or more directed edges, which we denote by  $\mathcal{C} \in \mathbb{C}_{\mathcal{L}}$ , where  $\mathcal{C}$  is the set of the directed edges contained in the cycle.

By disjoint we mean that the above mentioned components do not have vertices in common, and we can write this informally as  $\mathcal{L} = \mathbb{C}_{\mathcal{L}} \cup \mathbb{S}_{\mathcal{L}} \cup \mathbb{E}_{\mathcal{L}}$  with  $\mathbb{C}_{\mathcal{L}}$ ,  $\mathbb{S}_{\mathcal{L}}$  and  $\mathbb{E}_{\mathcal{L}}$  mutually disjoint sets. A linear subgraph  $\mathcal{L}$  is *spanning* if all nodes of the original graph are contained in  $\mathcal{L}$ .

Having partitioned spanning linear subgraphs  $\mathcal{L}$  into three types of components, we can rewrite the sum in (C.2) as

$$\begin{aligned} & \det(\tilde{\mathbf{q}}(a) - \xi \mathbb{1}) \\ &= \sum_{\mathcal{L}} (-1)^{|\mathcal{X}| + \kappa(\mathcal{L})} \\ & \times \left( \prod_{(x \rightarrow x) \in \mathbb{S}_{\mathcal{L}}} (\tilde{\mathbf{q}}_{xx} - \xi) \right) \left( \prod_{\{(x \rightarrow y), (y \rightarrow x)\} \in \mathbb{E}_{\mathcal{L}}} \tilde{\mathbf{q}}_{yx} \tilde{\mathbf{q}}_{xy} \right) \left( \prod_{\mathcal{C} \in \mathbb{C}_{\mathcal{L}}} \prod_{(x \rightarrow y) \in \mathcal{C}} \tilde{\mathbf{q}}_{yx} \right). \quad (\text{C.3}) \end{aligned}$$

## C.3 Coefficients of directed cycles

The directed cycles  $\mathcal{C}$  that have more than three edges are defined by an ordered sequence  $\mathcal{C} = [x_1, x_2, \dots, x_{n(\mathcal{C})}, x_1]$  of nodes in  $\mathcal{X}$ , such that  $\tilde{\mathbf{q}}_{x_i x_{i+1}} \neq 0$  for all  $i$  and each vertex is only traversed once. Notice that directed cycles are similar to cycles in undirected graphs, as

defined in Sec C.1, but reversing the order of the nodes in a cycle  $\mathcal{C}$  does not give the same cycle, as we are considering a directed graph.

We associate to each directed cycle  $\mathcal{C}$  the coefficient

$$c_{\mathcal{C}} = \sum_{(x \rightarrow y) \in \mathcal{C}} c_{xy}. \quad (\text{C.4})$$

In what follows, we show that the coefficients  $c_{\mathcal{C}}$  can be expressed as a linear combination of the coefficients  $c_{\gamma}$  with  $\gamma \in \mathcal{C}$ , the fundamental cycle basis. To this aim, we associate to each  $\gamma$  two directed cycles,  $\mathcal{C}_{\gamma}^{+}$  and  $\mathcal{C}_{\gamma}^{-}$ , which traverse the nodes of  $\gamma$  in opposing directions. It then follows from the definition (C.4) and the fact that  $c_{xy} = -c_{yx}$  that

$$c_{\mathcal{C}_{\gamma}^{+}} = -c_{\mathcal{C}_{\gamma}^{-}} = c_{\gamma}, \quad (\text{C.5})$$

where we use the convention that  $c_{\mathcal{C}_{\gamma}^{+}} = c_{\gamma}$ . In fact, Eq. (C.5) extends to any cycle of a graph, and since  $\mathcal{C}$  is a fundamental cycle basis, any cycle is a symmetric difference of the cycles  $\gamma \in \mathcal{C}$ . Therefore, it holds

$$c_{\mathcal{C}} = \sum_{\gamma \in \mathcal{C}} \epsilon_{\mathcal{C}, \gamma} c_{\gamma}, \quad (\text{C.6})$$

where  $\epsilon_{\mathcal{C}, \gamma} \in \{-1, 0, 1\}$  are used to direction in which the cycles  $\gamma$  are traversed.

#### C.4 Characteristic polynomial of $\tilde{\mathbf{q}}(a)$ as a function of the $c_{\gamma}$

We use the definition of  $\tilde{\mathbf{q}}(a)$ , given by Eq. (13) in the main text, in the expression (C.3) for the characteristic polynomial. We consider each of the three products of Eq. (C.3) separately, and then we put them together.

For the self loops we get

$$\prod_{(x \rightarrow x) \in \mathbb{S}_{\mathcal{L}}} (\tilde{\mathbf{q}}_{xx} - \xi) = \prod_{(x \rightarrow x) \in \mathbb{S}_{\mathcal{L}}} (\mathbf{q}_{xx} - \xi), \quad (\text{C.7})$$

which does not depend on the  $c_{xy}$ .

For the cycles of length two, we get

$$\begin{aligned} \prod_{\{(x \rightarrow y), (y \rightarrow x)\} \in \mathbb{E}_{\mathcal{L}}} \tilde{\mathbf{q}}_{yx} \tilde{\mathbf{q}}_{xy} &= \prod_{\{(x \rightarrow y), (y \rightarrow x)\} \in \mathbb{E}_{\mathcal{L}}} \mathbf{q}_{xy} \exp(-ac_{xy}) \mathbf{q}_{yx} \exp(-ac_{yx}) \\ &= \prod_{\{(x \rightarrow y), (y \rightarrow x)\} \in \mathbb{E}_{\mathcal{L}}} \mathbf{q}_{yx} \mathbf{q}_{xy}, \end{aligned} \quad (\text{C.8})$$

where we have used  $c_{xy} = -c_{yx}$ , and hence also this product does not depend on  $c_{xy}$ .

Lastly, we consider the directed cycles of length three or larger. In this case we get

$$\prod_{\mathcal{C} \in \mathbb{C}_{\mathcal{L}}} \prod_{(x \rightarrow y) \in \mathcal{C}} \tilde{\mathbf{q}}_{yx} = \prod_{\mathcal{C} \in \mathbb{C}_{\mathcal{L}}} \left( \exp(-ac_{\mathcal{C}}) \prod_{(x \rightarrow y) \in \mathcal{C}} \mathbf{q}_{yx} \right), \quad (\text{C.9})$$

where we have used the definition (C.4) for  $c_{\mathcal{C}}$ .

Putting the Eqns. (C.8), (C.7), and (C.9) together, we can write the characteristic polynomial as

$$\begin{aligned} \det(\tilde{\mathbf{q}}(a) - \xi \mathbb{1}) &= \sum_{\mathcal{L}} (-1)^{|\mathcal{L}| + \kappa(\mathcal{L})} \left( \prod_{(x \rightarrow x) \in \mathbb{S}_{\mathcal{L}}} (\mathbf{q}_{xx} - \xi) \right) \left( \prod_{\{(x \rightarrow y), (y \rightarrow x)\} \in \mathbb{E}_{\mathcal{L}}} \mathbf{q}_{yx} \mathbf{q}_{xy} \right) \\ &\quad \times \left( \prod_{\mathcal{C} \in \mathbb{C}_{\mathcal{L}}} \exp(\mathcal{A}_{\mathcal{C}}) \exp(-ac_{\mathcal{C}}) \right), \end{aligned} \quad (\text{C.10})$$

where we have defined the “semi” affinity  $\mathcal{A}_{\mathcal{C}} = \ln \prod_{(x \rightarrow y) \in \mathcal{C}} \mathbf{q}_{yx}$ . Lastly, using (C.6) in (C.10) yields

$$\det(\tilde{\mathbf{q}}(a) - \xi \mathbb{1}) = \sum_{\mathcal{L}} (-1)^{|\mathcal{X}| + \kappa(\mathcal{L})} \left( \prod_{\mathbb{S}_{(x,x)} \in \mathcal{L}} (\mathbf{q}_{xx} - \xi) \right) \left( \prod_{\{(x \rightarrow y), (y \rightarrow x)\} \in \mathbb{E}_{\mathcal{L}}} \mathbf{q}_{yx} \mathbf{q}_{xy} \right) \left( \prod_{\mathcal{C} \in \mathbb{C}_{\mathcal{L}}} \exp(\mathcal{A}_{\mathcal{C}}) \exp\left(-a \sum_{\gamma \in \mathcal{C}} \epsilon_{\mathcal{C}, \gamma} c_{\gamma}\right) \right). \quad (\text{C.11})$$

From (C.11) we conclude that the characteristic polynomial is a function of the coefficients  $c_{\gamma}$  with  $\gamma \in \mathcal{C}$ .

Notice that if  $J_t = S_t$ , the stochastic entropy production, then  $c_{\mathcal{C}} = \mathcal{A}_{\mathcal{C}} - \mathcal{A}_{\tilde{\mathcal{C}}}$ , where  $\tilde{\mathcal{C}}$  is reverse of cycle  $\mathcal{C}$ , and thus  $c_{\mathcal{C}} = -c_{\tilde{\mathcal{C}}}$ . Using these coefficients (C.10) readily yields the Galavotti-Cohen symmetry [10], see also Ref. [47] for a detailed analysis.

## D Model parameters for Kinesin-1 model

The model of Figure 3 is the mechanochemical model for kinesin-1 from Ref. [52] with one minor modification, namely, we eliminated a unidirectional transition to an absorbing state, corresponding to the detachment of the motor from the biofilament. The graph in Fig.3(a) shows the nonzero offdiagonal entries of the  $\mathbf{q}$ -matrix. Functional dependence of the rates as a function of the concentration [ATP] of adenosine triphosphate (ATP), the mechanical force  $f$  opposing motion of the motor towards the positive end of the microtubule, the Boltzmann constant  $k_B$ , the temperature  $T_{\text{env}}$ , and the so-called load distribution factors  $\delta$  are given by

- $\mathbf{q}_{12} = \mathbf{q}_{12}^0 [\text{ATP}]$ ,
- $\mathbf{q}_{13} = \mathbf{q}_{13}^0 \exp\left(\delta_{13} \frac{fd}{k_B T_{\text{env}}}\right)$ ,
- $\mathbf{q}_{15} = \mathbf{q}_{15}^0$ ,
- $\mathbf{q}_{21} = \mathbf{q}_{21}^0$ ,
- $\mathbf{q}_{23} = \mathbf{q}_{23}^0 \exp\left(-\delta_{23} \frac{fd}{k_B T_{\text{env}}}\right)$ ,
- $\mathbf{q}_{24} = \mathbf{q}_{24}^0 \exp\left(\delta_{24} \frac{fd}{k_B T_{\text{env}}}\right)$ ,
- $\mathbf{q}_{25} = \mathbf{q}_{25}^0$ ,
- $\mathbf{q}_{31} = \mathbf{q}_{31}^0 \exp\left(-\delta_{31} \frac{fd}{k_B T_{\text{env}}}\right)$ ,
- $\mathbf{q}_{32} = \mathbf{q}_{32}^0 \exp\left(\delta_{32} \frac{fd}{k_B T_{\text{env}}}\right)$ ,
- $\mathbf{q}_{34} = \mathbf{q}_{34}^0 [\text{ATP}]$ ,
- $\mathbf{q}_{42} = \mathbf{q}_{42}^0 \exp\left(-\delta_{42} \frac{fd}{k_B T_{\text{env}}}\right)$ ,
- $\mathbf{q}_{43} = \mathbf{q}_{43}^0$ ,
- $\mathbf{q}_{51} = \mathbf{q}_{51}^0$ ,
- $\mathbf{q}_{52} = \mathbf{q}_{52}^0$ .

The numerical values chosen for the above parameters are

- $\mathbf{q}_{34}^0 = \mathbf{q}_{12}^0 = 9.827 \mu\text{M}^{-1}$ ,
- $\mathbf{q}_{43}^0 = \mathbf{q}_{21}^0 = 5047.875$ ,

- $\mathbf{q}_{23}^0 = 1627.099$ ,
- $\mathbf{q}_{32}^0 = 0.006$ ,
- $\mathbf{q}_{24}^0 = \mathbf{q}_1^0 = 1.666$ ,
- $\mathbf{q}_{42}^0 = \mathbf{q}_{31}^0 = 137.582$ ,
- $\mathbf{q}_{15}^0 = 4.344$ ,
- $\mathbf{q}_{51}^0 = 345.215$ ,
- $\mathbf{q}_{25}^0 = 5146.371$ ,
- $\mathbf{q}_{52}^0 = 77.252$ ,
- $[ATP] = 1\mu M$ .

The temperature  $T_{\text{env}} = 296 K$  and the Boltzmann constant  $k_B = 1.3806 \times 10^{-23} J/K$ .

The load distribution parameters  $\delta_{xy}$  are given by  $\delta_{13} = 0.529$ ,  $\delta_{31} = 0$ ,  $\delta_{23} = 0.055$ ,  $\delta_{32} = 0.416$ ,  $\delta_{42} = 0.006$ ,  $\delta_{24} = 0.523$ . Note that these parameters sum to one in a cycle, i.e.  $\delta_{24} + \delta_{42} + \delta_{23} + \delta_{32} = \delta_{13} + \delta_{31} + \delta_{23} + \delta_{32} = 1$ .

The positional current  $J_t$  of the kinesin-1 motor protein is a fluctuating current determined by the coefficients

- $c_{13} = -c_{31} = (\delta_{13} + \delta_{31})$ ,
- $c_{24} = -c_{42} = (\delta_{24} + \delta_{42})$ ,
- and  $c_{23} = -c_{32} = (\delta_{23} + \delta_{32})$ ,

with all other coefficients  $c_{xy}$  set to zero. One unit of distance travelled by the motor protein equals the length of one microtubule dimer, which is  $d = 8 nm$ . Hence, the distance travelled by kinesin-1 measured in nanometers is given by  $J_t d$ . In Figure 2b, the mechanical force  $f$  is a parameter that varies along the x-axis and is measured in piconewton (pN). With these parameters, the effective affinity  $a^*$  and  $\bar{j}$  were calculated by numerically diagonalizing  $\tilde{\mathbf{q}}(a)$  and  $\mathbf{q}$  respectively.

## E Difference between the effective affinity and the stalling force for currents that are not thermodynamically consistent

Figure 4 of Section 9.1 shows that thermodynamically consistent currents that satisfy the conditions (79) have an effective affinity that is approximately equal to the stalling force. In this Appendix, we show that for currents that are not thermodynamically consistent, the difference between the effective affinity and the stalling force can be large.

Indeed, in Fig. 6 we plot the difference between effective affinity  $a^*$  and the stalling force  $f_{\text{stall}}$  as a function of the force  $f$  for randomly chosen currents that violate the thermodynamic consistency condition in the model of Kinesin-1. As we can see, in contrast with the thermodynamically consistent case, the effective affinity differs significantly from the stalling force for currents that are not thermodynamically consistent.

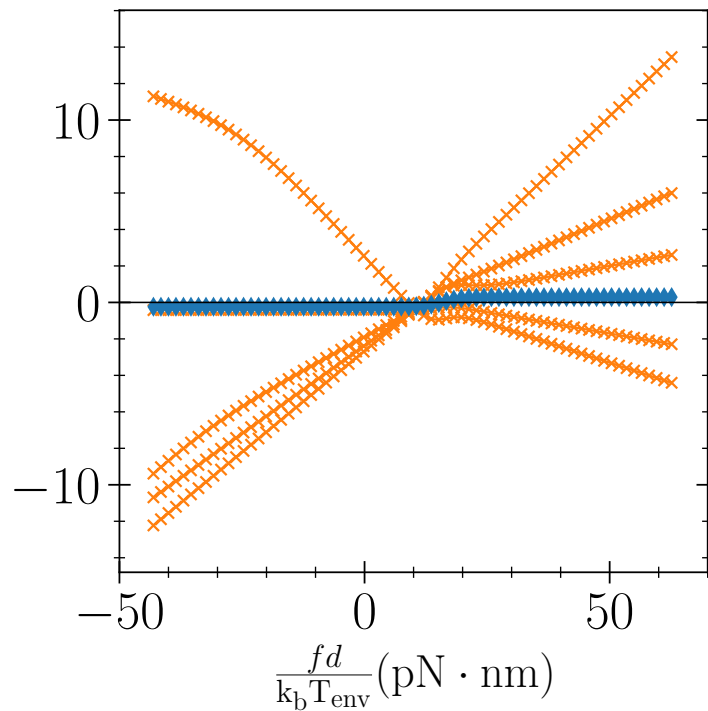


Figure 6: The yellow crosses in the plot above show  $(a^* - f_{\text{stall}})$  (i.e, the difference between the left and right hand sides of Eq. (69)) as a function of  $f$ , when thermodynamic consistency is broken in the model of Kinesin-1 depicted in Fig. 4(a). The different curves are for values of  $c_{31}$ ,  $c_{42}$  and  $c_{25}$  chosen randomly from a uniform distribution between 0 and 1. All other parameters are the same as listed in Appendix D. The blue diamonds show the same plot for the thermodynamically consistent case (as depicted in Fig. 5) for comparison.



## References

- [1] RB. Raffa and RJ. Tallarida, *'Affinity': Historical development in chemistry and pharmacology*, Bulletin for the History of Chemistry **35**(1), 7 (2010).
- [2] T. D. Donder, *L'affinité*, Gauthier-Villars, Paris (1927).
- [3] T. De Donder and P. Van Rysselberghe, *Thermodynamic Theory of Affinity*, Stanford university press (1936).
- [4] D. Kondepudi and I. Prigogine, *Modern Thermodynamics: From Heat Engines to Dissipative Structures*, John Wiley & Sons, New York, doi:[10.1002/9781118698723](https://doi.org/10.1002/9781118698723) (1998).
- [5] T. L. Hill, *Free Energy Transduction and Biochemical Cycle Kinetics*, Springer, New York, NY, ISBN 978-0-387-96836-0 978-1-4612-3558-3, doi:[10.1007/978-1-4612-3558-3](https://doi.org/10.1007/978-1-4612-3558-3) (1989).
- [6] J. Schnakenberg, *Network theory of microscopic and macroscopic behavior of master equation systems*, Reviews of Modern Physics **48**(4), 571 (1976), doi:[10.1103/RevModPhys.48.571](https://doi.org/10.1103/RevModPhys.48.571).
- [7] L. Peliti and S. Pigolotti, *Stochastic Thermodynamics: An Introduction*, Princeton University Press, doi:[10.1080/00107514.2024.2351562](https://doi.org/10.1080/00107514.2024.2351562) (2021).
- [8] C. Maes, *Local detailed balance*, SciPost Physics Lecture Notes **13004**, 032 (2021), doi:[10.1007/978-3-030-87672-2](https://doi.org/10.1007/978-3-030-87672-2).
- [9] P. Gaspard, *Multivariate fluctuation relations for currents*, New Journal of Physics **15**(11), 115014 (2013), doi:[10.1088/1367-2630/15/11/115014](https://doi.org/10.1088/1367-2630/15/11/115014).
- [10] J. L. Lebowitz and H. Spohn, *A Gallavotti–Cohen-type symmetry in the large deviation functional for stochastic dynamics*, Journal of Statistical Physics **95**(1/2), 333 (1999), doi:[10.1023/a:1004589714161](https://doi.org/10.1023/a:1004589714161).
- [11] U. Seifert, *Entropy production along a stochastic trajectory and an integral fluctuation theorem*, Physical Review Letters **95**(4), 040602 (2005), doi:[10.1103/PhysRevLett.95.040602](https://doi.org/10.1103/PhysRevLett.95.040602).
- [12] D. Andrieux and P. Gaspard, *Fluctuation theorem for currents and Schnakenberg network theory*, Journal of Statistical Physics **127**(1), 107 (2007), doi:[10.1007/s10955-006-9233-5](https://doi.org/10.1007/s10955-006-9233-5).
- [13] U. Seifert, *Stochastic thermodynamics, fluctuation theorems and molecular machines*, Reports on Progress in Physics **75**(12), 126001 (2012), doi:[10.1088/0034-4885/75/12/126001](https://doi.org/10.1088/0034-4885/75/12/126001).
- [14] D. Andrieux and P. Gaspard, *Network and thermodynamic conditions for a single macroscopic current fluctuation theorem*, Comptes Rendus Physique **8**(5-6), 579 (2007), doi:[10.1016/j.crhy.2007.04.016](https://doi.org/10.1016/j.crhy.2007.04.016).
- [15] G. Bulnes Cuetara, M. Esposito, G. Schaller and P. Gaspard, *Effective fluctuation theorems for electron transport in a double quantum dot coupled to a quantum point contact*, Physical Review B **88**(11), 115134 (2013), doi:[10.1103/PhysRevB.88.115134](https://doi.org/10.1103/PhysRevB.88.115134).
- [16] M. Polettini and M. Esposito, *Effective thermodynamics for a marginal observer*, Physical Review Letters **119**(24), 240601 (2017), doi:[10.1103/PhysRevLett.119.240601](https://doi.org/10.1103/PhysRevLett.119.240601).

- [17] G. Bisker, M. Poletini, T. R. Gingrich and J. M. Horowitz, *Hierarchical bounds on entropy production inferred from partial information*, *Journal of Statistical Mechanics: Theory and Experiment* **2017**(9), 093210 (2017), doi:[10.1088/1742-5468/aa8c0d](https://doi.org/10.1088/1742-5468/aa8c0d).
- [18] M. Poletini and M. Esposito, *Effective fluctuation and response theory*, *Journal of Statistical Physics* **176**(1), 94 (2019), doi:[10.1007/s10955-019-02291-7](https://doi.org/10.1007/s10955-019-02291-7).
- [19] I. Neri and M. Poletini, *Extreme value statistics of edge currents in Markov jump processes and their use for entropy production estimation*, *SciPost Physics* **14**(5), 131 (2023), doi:[10.21468/SciPostPhys.14.5.131](https://doi.org/10.21468/SciPostPhys.14.5.131).
- [20] C. Battle, C. P. Broedersz, N. Fakhri, V. F. Geyer, J. Howard, C. F. Schmidt and F. C. MacKintosh, *Broken detailed balance at mesoscopic scales in active biological systems*, *Science* **352**(6285), 604 (2016), doi:[10.1126/science.aac8167](https://doi.org/10.1126/science.aac8167).
- [21] I. Di Terlizzi, M. Gironella, D. Herraes-Aguilar, T. Betz, F. Monroy, M. Baiesi and F. Ritort, *Variance sum rule for entropy production*, *Science* **383**(6686), 971 (2024), doi:[10.1126/science.adh1823](https://doi.org/10.1126/science.adh1823).
- [22] K. Sekimoto, *Stochastic Energetics*, Springer Berlin Heidelberg, ISBN 978-3-642-05411-2, doi:[10.1007/978-3-642-05411-2\\_7](https://doi.org/10.1007/978-3-642-05411-2_7) (2010).
- [23] M. Poletini and M. Esposito, *Transient fluctuation theorems for the currents and initial equilibrium ensembles*, *Journal of Statistical Mechanics: Theory and Experiment* **2014**(10), P10033 (2014), doi:[10.1088/1742-5468/2014/10/P10033](https://doi.org/10.1088/1742-5468/2014/10/P10033).
- [24] I. Neri, É. Roldán and F. Jülicher, *Statistics of infima and stopping times of entropy production and applications to active molecular processes*, *Physical Review X* **7**(1), 011019 (2017), doi:[10.1103/PhysRevX.7.011019](https://doi.org/10.1103/PhysRevX.7.011019).
- [25] I. Neri, É. Roldán, S. Pigolotti and F. Jülicher, *Integral fluctuation relations for entropy production at stopping times*, *Journal of Statistical Mechanics: Theory and Experiment* **2019**(10), 104006 (2019), doi:[10.1088/1742-5468/ab40a0](https://doi.org/10.1088/1742-5468/ab40a0).
- [26] R. Chetrite and S. Gupta, *Two refreshing views of fluctuation theorems through kinematics elements and exponential martingale*, *Journal of Statistical Physics* **143**(3), 543 (2011), doi:[10.1007/s10955-011-0184-0](https://doi.org/10.1007/s10955-011-0184-0).
- [27] I. Neri, *Universal tradeoff relation between speed, uncertainty, and dissipation in nonequilibrium stationary states*, *SciPost Physics* **12**(4), 139 (2022), doi:[10.21468/SciPostPhys.12.4.139](https://doi.org/10.21468/SciPostPhys.12.4.139).
- [28] J. R. Norris, *Markov Chains*, vol. 2 of *Cambridge Series on Statistical and Probabilistic Mathematics*, Cambridge University Press, New York, NY, USA, doi:[10.1017/cbo9780511810633](https://doi.org/10.1017/cbo9780511810633) (1997).
- [29] T. Liggett, *Continuous Time Markov Processes: An Introduction*, Graduate Studies in Mathematics. American Mathematical Society, ISBN 978-0-8218-4949-1, doi:[10.1090/gsm/113](https://doi.org/10.1090/gsm/113) (2010).
- [30] P. Brémaud, *Markov Chains: Gibbs Fields, Monte Carlo Simulation, and Queues*, vol. 31, Springer Science & Business Media, doi:[10.1007/978-3-030-45982-6](https://doi.org/10.1007/978-3-030-45982-6) (2013).
- [31] C. Maes, K. Netočný and B. Wynants, *Steady state statistics of driven diffusions*, *Physica A: Statistical Mechanics and its Applications* **387**(12), 2675 (2008), doi:[10.1016/j.physa.2008.01.097](https://doi.org/10.1016/j.physa.2008.01.097).

- [32] C. Maes and K. Netočný, *Canonical structure of dynamical fluctuations in mesoscopic nonequilibrium steady states*, EPL (Europhysics Letters) **82**(3), 30003 (2008), doi:[10.1209/0295-5075/82/30003](https://doi.org/10.1209/0295-5075/82/30003).
- [33] L. Bertini, A. Faggionato and D. Gabrielli, *Flows, currents, and cycles for Markov chains: Large deviation asymptotics*, Stochastic Processes and their Applications **125**(7), 2786 (2015), doi:[10.1016/j.spa.2015.02.001](https://doi.org/10.1016/j.spa.2015.02.001).
- [34] H. Touchette, *The large deviation approach to statistical mechanics*, Physics Reports **478**(1-3), 1 (2009), doi:[10.1016/j.physrep.2009.05.002](https://doi.org/10.1016/j.physrep.2009.05.002).
- [35] A. Dembo and O. Zeitouni, *Large Deviations Techniques and Applications*, Springer, Berlin Heidelberg, doi:[10.1007/978-1-4612-5320-4](https://doi.org/10.1007/978-1-4612-5320-4) (2010).
- [36] P. Pietzonka, A. C. Barato and U. Seifert, *Universal bounds on current fluctuations*, Physical Review E **93**(5), 052145 (2016), doi:[10.1103/PhysRevE.93.052145](https://doi.org/10.1103/PhysRevE.93.052145).
- [37] T. R. Gingrich, J. M. Horowitz, N. Perunov and J. L. England, *Dissipation bounds all steady-state current fluctuations*, Physical Review Letters **116**(12), 120601 (2016), doi:[10.1103/PhysRevLett.116.120601](https://doi.org/10.1103/PhysRevLett.116.120601).
- [38] R. Chetrite and H. Touchette, *Nonequilibrium Markov Processes Conditioned on Large Deviations*, Annales Henri Poincaré **16**(9), 2005 (2015), doi:[10.1007/s00023-014-0375-8](https://doi.org/10.1007/s00023-014-0375-8).
- [39] É. Roldán, I. Neri, R. Chetrite, S. Gupta, S. Pigolotti, F. Jülicher and K. Sekimoto, *Martingales for physicists: A treatise on stochastic thermodynamics and beyond*, Advances in Physics **72**(1-2), 1 (2023), doi:[10.1080/00018732.2024.2317494](https://doi.org/10.1080/00018732.2024.2317494).
- [40] K. Devlin, *The Unfinished Game: Pascal, Fermat, and the Seventeenth-Century Letter That Made the World Modern*, Basic Books (2010).
- [41] C. Huygens, *Van Rekeningh in Spelen van Geluck*, Epsilon Uitgaven (1998).
- [42] F. Avanzini, M. Bilancioni, V. Cavina, S. Dal Cengio, M. Esposito, G. Falasco, D. Forastiere, J. N. Freitas, A. Garilli, P. E. Harunari *et al.*, *Methods and conversations in (post) modern thermodynamics*, chap. 9. SciPost Physics Lecture Notes, doi:[10.21468/SciPostPhysLectNotes.80](https://doi.org/10.21468/SciPostPhysLectNotes.80) (2024).
- [43] D. Williams, *Probability with Martingales*, Cambridge university press, doi:[10.1017/cbo9780511813658](https://doi.org/10.1017/cbo9780511813658) (1991).
- [44] A. Wald, *Some generalizations of the theory of cumulative sums of random variables*, The Annals of Mathematical Statistics **16**(3), 287 (1945), doi:[10.1214/aoms/1177731092](https://doi.org/10.1214/aoms/1177731092).
- [45] A. Wald, *On cumulative sums of random variables*, The Annals of Mathematical Statistics **15**(3), 283 (1944), doi:[10.1214/aoms/1177731235](https://doi.org/10.1214/aoms/1177731235).
- [46] I. Neri, *Estimating entropy production rates with first-passage processes*, Journal of Physics A: Mathematical and Theoretical **55**(30), 304005 (2022), doi:[10.1088/1751-8121/ac736b](https://doi.org/10.1088/1751-8121/ac736b).
- [47] A. C. Barato and R. Chetrite, *On the symmetry of current probability distributions in jump processes*, Journal of Physics A: Mathematical and Theoretical **45**(48), 485002 (2012), doi:[10.1088/1751-8113/45/48/485002](https://doi.org/10.1088/1751-8113/45/48/485002).

- [48] B. D. Acharya, *Spectral criterion for cycle balance in networks*, Journal of Graph Theory **4**(1), 1 (1980), doi:[10.1002/jgt.3190040102](https://doi.org/10.1002/jgt.3190040102).
- [49] K. Proesmans and B. Derrida, *Large-deviation theory for a Brownian particle on a ring: A WKB approach*, Journal of Statistical Mechanics: Theory and Experiment **2019**(2), 023201 (2019), doi:[10.1088/1742-5468/aafa7e](https://doi.org/10.1088/1742-5468/aafa7e).
- [50] S. Pigolotti, I. Neri, É. Roldán and F. Jülicher, *Generic properties of stochastic entropy production*, Physical Review Letters **119**(14), 140604 (2017), doi:[10.1103/PhysRevLett.119.140604](https://doi.org/10.1103/PhysRevLett.119.140604).
- [51] S. Liepelt and R. Lipowsky, *Kinesin's network of chemomechanical motor cycles*, Physical Review Letters **98**(25), 258102 (2007), doi:[10.1103/PhysRevLett.98.258102](https://doi.org/10.1103/PhysRevLett.98.258102).
- [52] B. Shen and Y. Zhang, *A mechanochemical model of the forward/backward movement of motor protein kinesin-1*, Journal of Biological Chemistry **298**(6), 101948 (2022), doi:[10.1016/j.jbc.2022.101948](https://doi.org/10.1016/j.jbc.2022.101948).
- [53] C. M. Coppin, J. T. Finer, J. A. Spudich and R. D. Vale, *Detection of sub-8-nm movements of kinesin by high-resolution optical-trap microscopy.*, Proceedings of the National Academy of Sciences **93**(5), 1913 (1996), doi:[10.1073/pnas.93.5.1913](https://doi.org/10.1073/pnas.93.5.1913).
- [54] M. Nishiyama, E. Muto, Y. Inoue, T. Yanagida and H. Higuchi, *Substeps within the 8-nm step of the ATPase cycle of single kinesin molecules*, Nature Cell Biology **3**(4), 425 (2001), doi:[10.1038/35070116](https://doi.org/10.1038/35070116).
- [55] P. E. Harunari, A. Garilli and M. Polettini, *Beat of a current*, Physical Review E **107**(4), L042105 (2023), doi:[10.1103/PhysRevE.107.L042105](https://doi.org/10.1103/PhysRevE.107.L042105).
- [56] A. Garilli, P. E. Harunari and M. Polettini, *Fluctuation relations for a few observable currents at their own beat*, arXiv preprint arXiv:2312.07505 (2023), doi:[10.48550/arXiv.2312.07505](https://doi.org/10.48550/arXiv.2312.07505), [2312.07505](https://arxiv.org/abs/2312.07505).
- [57] P. E. Harunari, A. Dutta, M. Polettini and É. Roldán, *What to Learn from a Few Visible Transitions' Statistics?*, Physical Review X **12**(4), 041026 (2022), doi:[10.1103/PhysRevX.12.041026](https://doi.org/10.1103/PhysRevX.12.041026).
- [58] H. Qian, *Vector field formalism and analysis for a class of thermal ratchets*, Physical review letters **81**(15), 3063 (1998), doi:[10.1103/PhysRevLett.81.3063](https://doi.org/10.1103/PhysRevLett.81.3063).
- [59] Y.-J. Yang and H. Qian, *Bivectorial nonequilibrium thermodynamics: Cycle affinity, vorticity potential, and Onsager's principle*, Journal of Statistical Physics **182**, 1 (2021), doi:[10.1007/s10955-021-02723-3](https://doi.org/10.1007/s10955-021-02723-3).
- [60] A. Berman and R. Plemmons, *Nonnegative Matrices in the Mathematical Sciences*, vol. 9 of *Classics in Applied Mathematics*, Society for Industrial and Applied Mathematics, ISBN 978-0-89871-321-3, doi:[10.1137/1.9781611971262](https://doi.org/10.1137/1.9781611971262) (1994).
- [61] B. Bollobás, *Modern Graph Theory*, Springer Science & Business Media, ISBN 978-0-387-98488-9, doi:[10.1007/978-1-4612-0619-4](https://doi.org/10.1007/978-1-4612-0619-4) (1998).
- [62] D. M. Cvetković, M. Doob and H. Sachs, *Spectra of Graphs: Theory and Applications*, Johann Ambrosius Barth (1995).